



## **SISALv2: A comprehensive speleothem isotope database with multiple age-depth models**

Laia Comas-Bru 1, Kira Rehfeld 2, Carla Roesch 2, Sahar Amirnezhad-Mozhdehi 3, Sandy P. Harrison 1, Kamolphet Atsawawanunt 1, Syed Masood Ahmad 4, Yassine Ait Brahim 5, Andy Baker 6, Matthew Bosomworth 1, Sebastian F.M. Breitenbach 7, Yuval Burstyn 8, Andrea Columbu 9, Michael Deininger 10, Attila Demény 11, Bronwyn Dixon 12, Jens Fohlmeister 13, István Gábor Hatvani 11, Jun Hu 14, Nikita Kaushal 15, Zoltán Kern 11, Inga Labuhn 16, Franziska A. Lechleitner 17, Andrew Lorrey 18, Belen Martrat 19, Valdir Felipe Novello 20, Jessica Oster 21, Carlos Pérez-Mejías 5, Denis Scholz 10, Nick Scroton 22, Nitesh Sinha 23, Brittany Marie Ward 24, Sophie Warken 25, Haiwei Zhang 5 and SISAL Working Group members\*.

Correspondence: Laia Comas-Bru (l.comasbru@reading.ac.uk)

### **Affiliations:**

- 1 School of Archaeology, Geography, and Environmental Science, University of Reading, UK
- 2 Institute of Environmental Physics and Interdisciplinary Center for Scientific Computing, Heidelberg University, Germany
- 3 School of Geography, University College Dublin, Belfield, Dublin 4, Ireland
- 4 Department of Geography, Faculty of Natural Sciences, Jamia Millia Islamia, New Delhi, India
- 5 Institute of Global Environmental Change, Xi'an Jiaotong University, Xi'an, Shaanxi, China
- 6 Connected Waters Initiative Research Centre, UNSW Sydney, Sydney, New South Wales 2052, Australia
- 7 Department of Geography and Environmental Sciences, Northumbria University, Newcastle upon Tyne, UK
- 8 The Fredy & Nadine Herrmann Institute Earth Sciences, The Hebrew University of Jerusalem, The Edmond J. Safra Campus, Jerusalem 9190401, Israel
- 9 Department of Biological, Geological and Environmental Sciences (BiGeA), University of Bologna, Via Zamboni 67, 40126, Bologna, Italy
- 10 Institute for Geosciences, Johannes Gutenberg University Mainz, J.-J.-Becher-Weg 21, 55128 Mainz, Germany
- 11 Institute for Geological and Geochemical Research, Research Centre for Astronomy and Earth Sciences, H-1112, Budaörsi út 45, Budapest, Hungary
- 12 School of Geography, University of Melbourne, Australia; School of Archaeology, Geography, and Environmental Science, University of Reading, UK
- 13 Potsdam Institute for Climate Impact Research PIK, Potsdam, Germany
- 14 Department of Earth, Environmental and Planetary Sciences, Rice University, US
- 15 Asian School of the Environment, Nanyang Technological University, Singapore
- 16 Institute of Geography, University of Bremen, Celsiusstraße 2, 28359 Bremen, Germany
- 17 Department of Earth Sciences, South Parks Road, Oxford OX1 3AN, UK
- 18 National Institute of Water and Atmospheric Research, Auckland, 1010, New Zealand
- 19 Department of Environmental Chemistry, Spanish Council for Scientific Research (CSIC), Institute of Environmental Assessment and Water Research (IDAEA), Barcelona, Spain
- 20 Institute of Geoscience, University of São Paulo
- 21 Department of Earth and Environmental Sciences, Vanderbilt University, Nashville, TN 37240, US



22 School of Earth Sciences, University College Dublin, Belfield, Dublin 4, Ireland  
23 IBS Center for Climate Physics (ICCP), Pusan National University, South Korea  
24 Environmental Research Institute, University of Waikato, Hamilton, New Zealand  
25 Institute of Earth Sciences and Institute of Environmental Physics, Heidelberg University, Germany  
\* A full list of authors appears at the end of the paper.

1 **Abstract:**

2 Characterising the temporal uncertainty in palaeoclimate records is crucial for analysing past climate  
3 change, for correlating climate events between records, for assessing climate periodicities, identifying  
4 potential triggers, and to evaluate climate model simulations. The first global compilation of speleothem  
5 isotope records by the SISAL (Speleothem Isotope Synthesis and Analysis) Working Group showed that  
6 age-model uncertainties are not systematically reported in the published literature and these are only  
7 available for a limited number of records (ca. 15%,  $n = 107/691$ ). To improve the usefulness of the SISAL  
8 database, we have (i) improved the database's spatio-temporal coverage and (ii) created new  
9 chronologies using seven different approaches for age-depth modelling. We have applied these  
10 alternative chronologies to the records from the first version of the SISAL database (SISALv1) and to new  
11 records compiled since the release of SISALv1. This paper documents the necessary changes in the  
12 structure of the SISAL database to accommodate the inclusion of the new age-models and their  
13 uncertainties as well as the expansion of the database to include new records and the quality-control  
14 measures applied. This paper also documents the age-depth model approaches used to calculate the new  
15 chronologies. The updated version of the SISAL database (SISALv2) contains isotopic data from 691  
16 speleothem records from 294 cave sites and new age-depth models, including age-depth temporal  
17 uncertainties for 512 speleothems. SISALv2 is available at <http://dx.doi.org/10.17864/1947.242> (Comas-  
18 Bru et al., 2020).

19 **Copyright statement:** This dataset is licensed by the rights-holder(s) under a Creative Commons Attribution 4.0  
20 International Licence: <https://creativecommons.org/licenses/by/4.0/>

21 **1. Introduction**

22 Speleothems (secondary cave carbonates form from infiltrating rainwater after it percolates through the  
23 soil, epikarst, and carbonate bedrock) are a rich terrestrial palaeoclimate archive. In particular, stable  
24 oxygen and carbon isotopes ( $\delta^{18}\text{O}$ ,  $\delta^{13}\text{C}$ ) have been widely used to reconstruct regional and local  
25 hydroclimate changes. The Speleothem Isotope Synthesis and Analyses (SISAL) Working Group is an  
26 international effort, under the auspices of Past Global Changes (PAGES), to compile speleothem isotopic  
27 records globally for the analysis of past climates (Comas-Bru and Harrison, 2019). The first version of the  
28 SISAL database (Atsawawaranunt et al., 2018a; Atsawawaranunt et al., 2018b) contained 381 speleothem  
29 records from 174 cave sites and has been used for analysing regional climate changes (Braun et al., 2019a;



30 Burstyn et al., 2019; Comas-Bru and Harrison, 2019; Deininger et al., 2019; Kaushal et al., 2018; Kern et  
31 al., 2019; Lechleitner et al., 2018; Oster et al., 2019; Zhang et al., 2019). The potential for using the SISAL  
32 database to evaluate climate models was explored using an updated version of the database (SISALv1b;  
33 Atsawawanunt et al., 2019) that contains 455 speleothem records from 211 sites (Comas-Bru et al.,  
34 2019).

35 SISAL is continuing to expand the global database by including new records (Comas-Bru et al., 2020).  
36 Although most of the records in SISALv2 (79.7%: Figure 1a) have been dated using the generally very  
37 precise, absolute radiometric  $^{230}\text{Th}/\text{U}$  dating method, a variety of age-modelling approaches were  
38 employed (Figure 1b) in constructing the original records. The vast majority of records provide no  
39 information on the uncertainty of the age-depth relationship. However, many of the regional studies using  
40 SISAL pointed the limited statistical power of analyses of speleothem records because of the lack of  
41 temporal uncertainties. For example, these missing uncertainties prevented the extraction of underlying  
42 climate modes during the last 2k years in Europe (Lechleitner et al., 2018). To overcome this limitation,  
43 we have developed additional age-depth models for the SISALv2 records (Figure 2) in order to provide  
44 robust chronologies with temporal uncertainties. The results of the various age-depth modelling  
45 approaches differ because of differences in their underlying assumptions. We have used seven alternative  
46 methods: linear interpolation, linear regression, Bchron (Haslett and Parnell, 2008), Bacon (Blaauw, 2010;  
47 Blaauw and Christen, 2011; Blaauw et al., 2019), OxCal (Bronk Ramsey, 2008, 2009; Bronk Ramsey and  
48 Lee, 2013), COPRA (Breitenbach et al., 2012) and StalAge (Scholz and Hoffmann, 2011). Comparison of  
49 these different approaches provides a robust measure of the age uncertainty associated with any specific  
50 speleothem record.

## 51 **2. Data and Methods**

### 52 **2.1 Construction of age-depth models: the SISAL chronology**

53 We attempted to construct age-depth models for 533 entities in an automated mode. For eight records,  
54 this automated construction failed for all methods. For these records we provide manually constructed  
55 chronologies, where no age model previously existed, and added a note in the database with details on  
56 the construction procedure. Age models for 21 records were successfully computed but later dropped in  
57 the screening process due to inconsistent information or incompatibility for an automated routine. In  
58 total, we provide a new chronology for 512 speleothem records in SISALv2.

59 The SISAL chronology provides alternative age-depth models for SISAL records that are not composites  
60 (i.e., time-series based on more than one speleothem record), that have not been superseded in the



61 database by a newer entity and which are purely  $^{230}\text{Th}/\text{U}$  dated. We therefore excluded records for which  
62 the chronology is based on lamina counting, radiocarbon ages or a combination of methods. This decision  
63 was based on the low uncertainties of the age-depth models based on lamina counting and the challenge  
64 of reproducing age-depth models based on radiocarbon ages. We made an exception with the case of  
65 entity\_id 163 (Talma et al., 1992), which covers two key periods, the Mid-Holocene and the Last Glacial  
66 Maximum, at high temporal resolution. In this case, we calculated a new SISAL chronology based on the  
67 provided  $^{230}\text{Th}/\text{U}$  dates but did not consider the uncorrected  $^{14}\text{C}$  ages upon which the original age-depth  
68 model is based. We also excluded records for which isotopic data is not available (i.e., entities that are  
69 part of composites) and entities that are constrained by less than three dates. Additionally, the dating  
70 information for 23 entities shows hiatuses at the top/bottom of the speleothem that are not constrained  
71 by any date. For these records, we partially masked the new chronologies to remove the unconstrained  
72 section(s). Original dates were used without modification in the age-depth modelling.

73 To allow a comprehensive cross-examination of uncertainties, seven age-depth modelling techniques  
74 were implemented here across all selected records. Due to the high number of records ( $n = 533$ ), all  
75 methods were run in batch mode. A preliminary study, using the database version v1b demonstrated the  
76 feasibility of the automated construction and evaluation of age-depth models using a subset of records  
77 and methods (Roesch and Rehfeld, 2019). Further details on the evaluation of the updated age-depth  
78 models are provided in Section 3.2. The seven different methods are briefly described below. All methods  
79 assume that growth occurred along a single growth axis. For one entity, where it was previously known  
80 that two growth axes exist, we added an explanatory statement in the database. All approaches except  
81 StalAge produce Monte Carlo (MC) iterations of the age-depth models. We provide 1,000 MC iterations  
82 for each new SISALv2 chronology (<https://doi.org/10.5281/zenodo.3591197>).

83 Major challenges arise through hiatuses (growth interruptions) and age reversals. In the classification of  
84 the reversals, we distinguish between tractable reversals (with overlapping confidence intervals) and non-  
85 tractable reversals (i.e., where the two-sigma-dating uncertainties do not overlap) following the definition  
86 of Breitenbach et al. (2012). We developed a workflow to treat records with hiatuses (Roesch and Rehfeld,  
87 2019; details below), which allowed the construction of age-depth models for 20% of the records with  
88 one or more hiatuses. Changes, such as the hiatus treatment and outlier age modification, are recorded  
89 in a logfile created when running the age models. We followed the original author's choices with regard  
90 to date usage. If an age was marked as "not used" or "usage unknown", we did not consider this in the  
91 construction of the new chronologies except in OxCal, where dates with "usage unknown" were  
92 considered.



93 1) **Linear Interpolation** (*lin\_interp\_age*) between radiometric dates. This is the classic approach for age-  
94 depth model construction for palaeoclimate archives and was used in 32.1% of the original age-depth  
95 models in SISALv2. Here, we extend this approach and calculate the age uncertainty by sampling the range  
96 of uncertainty of each  $^{230}\text{Th}/\text{U}$ -age 2,000 times, assuming a Gaussian distribution. This is consistent with  
97 the implementation of linear interpolation in CLAM (Blaauw, 2010) and COPRA (Breitenbach et al., 2012).  
98 Linear interpolation was implemented in R (R Core Team, 2019), using the `approxExtrap()` function  
99 in the `Hmisc` package. We included an automated reversal check that increases the dating uncertainties  
100 until a monotonic age model is achieved, similar to that of `StalAge` (Scholz and Hoffmann, 2011). Hiatuses  
101 are modelled following the approach of Roesch and Rehfeld (2019), where rather than modelling each  
102 segment separately, synthetic ages with uncertainties spanning the entire hiatus duration are introduced  
103 for use in age-depth model construction. These synthetic ages are removed after age-depth model  
104 construction. Linear interpolation was applied to 80% ( $n=408/512$ ) of the SISAL records for which new  
105 chronologies were developed.

106 2) **Linear Regression** (*lin\_reg\_age*) provides a single best fit line through all available radiometric ages  
107 assuming a constant growth rate. Linear regression was used in 6.7% of the original SISALv2 age models.  
108 As with linear interpolation, age uncertainties are based on randomly sampling the U-series dates to  
109 produce 2,000 age-depth models (i.e., ensembles). Temporal uncertainties are then given by the  
110 uncertainty of the median-based fit to each ensemble member. If hiatuses are present, the segments in-  
111 between were split at the depth of the hiatus without an artificial age. The method is implemented in R,  
112 using the `lm()` function from the base package. Linear regression was applied to 36% ( $n=185/512$ ) of the  
113 SISAL records for which new chronologies were developed.

114 3) **Bchron** (*Bchron\_age*) is a Bayesian method based on a continuous Markov processes (Haslett and  
115 Parnell, 2008) and available as an R package (Parnell, 2018). This method was originally used for only one  
116 speleothem record in SISALv2. Since *Bchron* cannot handle hiatuses, we implemented a new workflow  
117 that adds synthetic ages with uncertainties spanning the entire hiatus duration (Roesch and Rehfeld,  
118 2019), as performed with linear interpolation, `StalAge` and our implementation of COPRA. *Bchron* provides  
119 age-depth model ensembles of which we have kept the last 2,000. Here we use the function `bchron()`  
120 with `jitter.positions = true` to mitigate problems due to rounded-off depth values. This  
121 method has been applied to 83% ( $n=426/512$ ) of the SISAL records for which new chronologies were  
122 developed.

123 4) **Bacon** (*Bacon\_age*) is a semi-parametric Bayesian method based on autoregressive gamma-processes  
124 (Blaauw, 2010; Blaauw and Christen, 2011; Blaauw et al., 2019). It was used in three of the original  
125 chronologies in SISALv2. The R package *rBacon* can handle both outliers and hiatuses and apart from



126 giving the median age-depth model, it also returns the Monte Carlo realisations (i.e. ensembles), from  
127 which the median age-depth model is calculated. During the creation of the SISAL chronologies, the  
128 existing *rBacon* package (version 2.3.9.1) was updated to improve the handling of stalagmite growth rates  
129 and hiatuses. We use this revised version, available on CRAN ([https://cran.r-](https://cran.r-project.org/web/packages/rbacon/index.html)  
130 [project.org/web/packages/rbacon/index.html](https://cran.r-project.org/web/packages/rbacon/index.html)), to provide a median age-depth model and an ensemble  
131 of age-model realisations for 65% (n=335/512) of the SISAL records for which new chronologies were  
132 developed.

133 5) **OxCal** (*Oxcal\_age*) is a Bayesian chronological modelling tool that uses Markov Chain Monte Carlo  
134 (Bronk Ramsey, 2009). This method was used in 4.1% of the original SISALv2 chronologies. OxCal can deal  
135 with hiatuses and outliers and accounts for the non-uniform nature of the deposition process (Poisson  
136 process using the `P_Sequence` command). Here we used the analysis module of OxCal version 4.3 with a  
137 default initial value of interpolation rate of 1 and an initial value of model rigidity ( $k$ ) of  $k_0=1$  with a uniform  
138 distribution from 0.01 to 100 for the range of  $k/k_0$  ( $\log_{10}(k/k_0)=(-2,2)$ ) (C. Bronk Ramsey, personal  
139 communication). The initial value of the interpolation rate determines the number of points between any  
140 two dates, for which an age will be calculated. We subsequently linearly interpolated the age-depth model  
141 to the depths of individual isotope measurements. Where multiple dates are given for the same depth for  
142 any given entity, the date with the smallest uncertainty was used to construct the SISAL chronology. In  
143 case of asymmetric uncertainties in the dating table, the largest uncertainty value was chosen. We kept  
144 the last 2,000 realisations of the age-depth models for each entity. OxCal chronologies are available for  
145 21% (n=106/512) of the SISAL records for which new chronologies were developed.

146 6) **COPRA** (*copRa\_age*) is an approach based on interpolation-between-dates (Breitenbach et al., 2012)  
147 and was used for 9.7% of the original SISALv2 chronologies. COPRA is available as a Matlab package with  
148 a graphical user interface (GUI) that has interactive checks for reversals and hiatuses. The Matlab version  
149 can handle multiple hiatuses and (to some extent) layer-counted segments. However, age-reversals can  
150 occur near short-lived hiatuses. To overcome this, we implemented a new workflow in  $\mathbb{R}$  that adds  
151 artificial dates at the location of the hiatuses and prevents the creation of age reversals (Roesch and  
152 Rehfeld, 2019) as done with linear interpolation, *StalAge* and *Bchron*. Additionally, we also incorporated  
153 an automated reversal check similar to that already embedded into *StalAge* (Scholz and Hoffmann, 2011).  
154 This  $\mathbb{R}$  version, *copRa*, uses the default piecewise-cubic-hermite-interpolation (`pchip`) algorithm in  $\mathbb{R}$   
155 without consideration of layer counting. This approach was used for 76% (n= 389/512) of the SISAL records  
156 for which new chronologies were developed.

157 7) **StalAge** (*StalAge\_age*) fits straight lines through three adjacent dates using weights based on the dating  
158 measurement errors (Scholz and Hoffmann, 2011). Age uncertainties are iteratively obtained through a



159 Monte Carlo approach, but ensembles are not given in the output. StalAge was used to construct 13.1%  
160 of the original SISALv2 chronologies. The StalAge v1.0 R function has been updated to R version 3.4 and  
161 the default outlier and reversal checks were enabled to run automatically. Hiatuses cannot be entered in  
162 StalAge v1.0, but the updated version incorporates a treatment of hiatuses based on the creation of  
163 temporary synthetic ages following Roesch and Rehfeld (2019). In contrast to other methods, mean ages  
164 instead of median ages are reported for StalAge. StalAge was applied to 62% (n=320/512) of the SISAL  
165 records for which new chronologies were developed.

## 166 2.2 Revised structure of the database

167 The data are stored in a relational database (MySQL), which consists of 15 linked tables: *site*, *entity*,  
168 *sample*, *dating*, *dating\_lamina*, *gap*, *hiatus*, *original\_chronology*, *d13C*, *d18O*, *entity\_link\_reference*,  
169 *references*, *composite\_link\_entity*, *notes* and *sisal\_chronology*. Figure 3 shows the relationships between  
170 these tables and the type of each field (e.g. numeric, text). The structure and contents of all tables except  
171 the new *sisal\_chronology* table are described in detail in Atsawawaranunt et al. (2018a). Here, we focus  
172 on the new *sisal\_chronology* table and on the changes that were made to other tables in order to  
173 accommodate this new table (See section 2.3). Details of the fields in this new table are listed in Table 1.

174 Changes were also made to the dating table (*dating*) to accommodate information about whether a  
175 specific date was used to construct each of the age-depth models in the *sisal\_chronology* table (Table 2).  
176 We followed the original authors' decision regarding the exclusion of dates (i.e. because of high  
177 uncertainties, age reversals or high detrital content). However, some dates used in the original age-depth  
178 model were not used in the SISALv2 chronologies to prevent unrealistic age-depth relationships (i.e. age  
179 inversions). Information on whether a particular date was used for the construction of specific type of  
180 age-depth model is provided in the dating table, under columns labelled *date\_used\_lin\_interp*,  
181 *date\_used\_lin\_reg*, *date\_used\_Bchron*, *date\_used\_Bacon*, *date\_used\_OxCal*, *date\_used\_copRa* and  
182 *date\_used\_StalAge* (Table 2).

183 The dating and the sample tables were modified to accommodate the inclusion of new entities in the  
184 database. Specifically, the pre-defined options lists were expanded, options that had never been used  
185 were removed, and some typographical errors in the field names were corrected; these changes are listed  
186 in Table 3.



### 187 3. Quality Control

#### 188 3.1 Quality control of individual speleothem records

189 The quality control procedure for individual records newly incorporated in the SISALv2 database is based  
190 on the steps described in Atsawawanunt et al. (2018a). We have updated the Python database scripts  
191 to provide a more thorough quality assessment of individual records. Additional checks of the dating table  
192 resulted in modifications in the *230Th\_232Th*, *230Th\_238U*, *234U\_238U*, *ini230Th\_232Th*, *238U\_content*,  
193 *230Th\_content*, *232Th\_content* and *decay constant* fields in the dating table for 60 entities. A summary  
194 of the fields that are both automatically and manually checked before uploading a record to the database  
195 is available in Appendix 1.

196 Analyses of the data included in SISALv1 (Braun et al., 2019a; Burstyn et al., 2019; Deininger et al., 2019;  
197 Kaushal et al., 2018; Kern et al., 2019; Lechleitner et al., 2018; Oster et al., 2019; Zhang et al., 2019) and  
198 SISALv1b (Comas-Bru et al., 2019) revealed a number of errors in specific records that have now been  
199 corrected. These revisions include, for example, updates in mineralogies (*sample.mineralogy*), revised  
200 coordinates (*site.latitude* and/or *site.longitude*) and addition of missing information that was previously  
201 entered as “unknown”. The fields affected and the number of records with modifications are listed in  
202 Table 4. All revisions are also documented at Comas-Bru et al., 2020.

#### 203 3.2 Quality control of the age-depth models in the SISAL chronology

204 The conception and the test of the R workflow, integrating all methods but OxCal, was outlined in Roesch  
205 and Rehfeld (2019) and includes automatized checks for the final chronologies except for OxCal. The  
206 quality control parameters obtained from OxCal were compared with the recommended values of  
207 Agreement Index (A) > 60% and Convergence (C) > 95%, in accordance with the guidelines in Bronk Ramsey  
208 (2008). In addition to both model agreement and P\_Sequence convergence meeting these criteria, at least  
209 90% of individual dates had to have an acceptable Agreement and Convergence themselves. OxCal age-  
210 depth models failing to meet these criteria were not included in the SISAL chronology table.

211 An overview of the evaluation results for the age-depth models constructed in automated mode is given  
212 in Figure 4. Three nested criteria are used to evaluate them. Firstly, chronologies with reversals (Check 1)  
213 are automatically rejected (score -1). Secondly, the final chronology should flexibly follow clear growth  
214 rate changes (Check 2), such that 70% of the dates are encompassed in the final age-depth model within  
215 4 sigma uncertainty (score +1). Thirdly, temporal uncertainties are expected to increase between dates  
216 and near hiatuses (Check 3). This criterion is met in the automated screening (score +1) if the Interquartile  
217 range (IQR) is higher between dates or at hiatuses than at dates. Only entities that pass all three criteria





218 are considered successful. All age-depth models that satisfied Check 1 were also evaluated in an expert-  
219 based manual screening by ten people. If more than two experts agreed that an individual age-depth  
220 model was unreliable or inconsistencies, such as large offsets between the original age model and the  
221 dates marked as 'used', occurred, the model was not included in the SISAL chronology table. This  
222 automatic and expert-based quality control screening resulted in 2,138 new age-depth models  
223 constructed for 503 SISAL entities.

#### 224 **4. Recommendation for the use of SISAL chronologies**

225 The original age-depth models for every entity are available in SISALv2. However, given the lack of age  
226 uncertainties for most of the records, we recommend considering the SISAL chronologies with their  
227 respective 95% confidence intervals whenever possible. No single age-depth modelling approach is  
228 successful for all entities, and we therefore recommend that all the methods for a specific entity are used  
229 together in visual and/or statistical comparisons. Depending on methodological choices, age-depth  
230 models compatible with the dating evidence can result in considerable temporal differences for  
231 transitions (Figure 5). For analyses relying on the temporal alignment of records (e.g. cross-correlation),  
232 age-depth model uncertainties should be considered using the ensemble of compatible age-depth models  
233 as described, e.g., in Mudelsee et al. (2012), Rehfeld and Kurths (2014) and Hu et al. (2017).

#### 234 **5. Overview of database contents**

235 SISALv2 contains 353,976  $\delta^{18}\text{O}$  and 200,613  $\delta^{13}\text{C}$  measurements from 673 individual speleothem records  
236 and 18 composite records from 293 cave systems (Table 5; Figure 2; Comas-Bru et al., 2020). There are 20  
237 records included in SISALv2 that are identified as being superseded and linked to the newer records; their  
238 original datasets are included in the database for completeness. This is an improvement of 235 records  
239 from SISALv1b (Atsawawaranunt et al., 2019; Comas-Bru et al., 2019; Table 6). SISALv2 represents 72% of  
240 the existing speleothem records identified by the SISAL Working Group and more than three times the  
241 number of speleothem records in the NCEI-NOAA repository ( $n = 210$  as of November 2019), which is the  
242 one most commonly used by the speleothem community to make their data publicly available. SISALv2  
243 also contains nine records that have not been published or are only available in PhD theses.

244 The published age-depth models of all speleothems are accessible in the *original\_chronology* metadata  
245 table and our standardised age-depth models are available at the *sisal\_chronology* table for 512  
246 speleothems. Temporal uncertainties are now provided for 79% of the records in the SISAL database.

247 This second version of the SISAL database has an improved spatial coverage compared to SISALv1  
248 (Atsawawaranunt et al., 2018b) and SISALv1b (Figure 3; Atsawawaranunt et al., 2019). SISALv2 contains



249 most published records from Oceania (80.2%), Africa (73.7%) and South America (77.6%), but  
250 improvements are still possible in regions like the Middle East (42.3%) and Asia (64.8%) (Table 6).

251 The temporal distribution of records for the past 2,000 years is good, with 181 speleothems covering at  
252 least one-third of this period and 84 records covering the entire last 2k (-68 to 2,000 years BP) with an  
253 average resolution of 20 isotope measurements in every 100-year slice (Figure 6a). There are 182 records  
254 that cover at least one-third of the Holocene (last 11,700 years BP) with 37 of these covering the whole  
255 period with at least one isotope measurement in every 500-year period (Figure 6b). There are 84 entities  
256 during the deglaciation period (21,000 to 11,700 years BP) with at least one measurement in every 500-  
257 year time period (Figure 6b). The Last Interglacial (130,000 to 115,000 years BP) is covered by 47  
258 speleothem records that record at least one-third of this period with, on average, 25 isotope  
259 measurements at every 1,000-year time-slice (Fig. 6c).

260 This updated SISALv2 database now provides the basis not only for comparing a large number of  
261 speleothem-based environmental reconstructions on regional to a global scale, but also allows for  
262 comprehensive analyses of stable isotope records on various timescales from multi-decadal to orbital.

## 263 **6. Data and code availability:**

264 The database is available in SQL and CSV format from <http://dx.doi.org/10.17864/1947.242> (Comas-Bru  
265 et al., 2020). The code used for constructing the linear interpolation, linear regression, Bchron, Bacon,  
266 copRa and StalAge age-depth models is available at <https://github.com/palaeovar/SISAL.AM>. *rBacon*  
267 package (version 2.3.9.1) is available on CRAN ([https://cran.r-  
268 project.org/web/packages/rbacon/index.html](https://cran.r-project.org/web/packages/rbacon/index.html)). The code used to construct the OxCal age-depth models  
269 and trim the ensembles output to the last 2,000 iterations is available at  
270 <https://doi.org/10.5281/zenodo.3586280>. The ensembles are available at  
271 <https://doi.org/10.5281/zenodo.3591197>. The workbook used to submit data to SISAL is available as a  
272 supplementary document of Comas-Bru and Harrison (2019); also available at  
273 <https://10.5281/zenodo.3631403>. The codes for the quality control assessment of the data submitted to  
274 SISAL can be obtained from <https://10.5281/zenodo.3631403>. The codes to assess the dating table in  
275 SISALv2 are available at [https://github.com/jensfohlmeister/QC\\_SISALv2\\_dating\\_metadata](https://github.com/jensfohlmeister/QC_SISALv2_dating_metadata) and  
276 <https://10.5281/zenodo.3631443>. Details on the Quality Control assessments are available in the  
277 Supplementary material.



278 **Author contributions:**

279 LCB is the coordinator of the SISAL working group. LCB, SPH and KR designed the new version of the  
280 database. KR coordinated the construction of the new age-depth models except OxCal. All age-depth  
281 models except OxCal were run by CR and KR. LCB coordinated the construction of the OxCal age-depth  
282 models, which were run by SAM and LCB. LCB implemented the changes in the v2 of the database with  
283 the assistance of KA. SMA, YAB, AB, YB, MB, AC, MD, AD, BD, IGH, JH, NK, ZK, FAL, AL, BM, VFN, JO, CPM,  
284 NS, NS, BMW, SW and HZ coordinated the regional data collection and the age-model screening. SFMB,  
285 MB and DS provided support for COPRA, Bacon and StalAge, respectively. JF assisted in the Quality Control  
286 procedure of the SISAL database. Figures 1, 4 and 5 were created by CR and KR. Figures 2, 3 and 6 were  
287 created by LCB. All authors listed as “SISAL Working Group members” provided data for this version of the  
288 database and/or helped to complete data entry. The first draft of the paper was written by LCB with inputs  
289 by KR and SPH and all authors contributed to the final version.

290 **Team list:**

291 The following SISAL Working Group members contributed with data to SISALv2: James Apaéstegui  
292 (Instituto Geofísico del Perú, Lima, Peru), Lisa M. Baldini (School of Health & Life Sciences, Teesside  
293 University, Middlesbrough, UK), Shraddha Band (Geoscience Department, National Taiwan University,  
294 No.1, Sec. 4, Roosevelt Road, Taipei 106, Taiwan), Maarten Blaauw (School of Natural and Built  
295 Environment, Queen's University Belfast, U.K.), Ronny Boch (Institute of Applied Geosciences, Graz  
296 University of Technology, Rechbauerstraße 12, 8010 Graz, Austria, Andrea Borsato (School of  
297 Environmental and Life Sciences, University of Newcastle, Callaghan 2308, NSW, Australia), Alexander  
298 Budsky (Institute for Geosciences, Johannes Gutenberg University Mainz, Johann-Joachim-Becher-Weg  
299 21, 55128 Mainz, Germany), Maria Gracia Bustamante Rosell (Department of Geology and Environmental  
300 Science, University of Pittsburgh, USA), Sakonvan Chawchai (Department of Geology, Faculty of Science,  
301 Chulalongkorn University, Bangkok 10330, Thailand), Silviu Constantin (Emil Racovita Institute of  
302 Speleology, Bucharest, Romania and Centro Nacional de Investigación sobre la Evolución Humana,  
303 CENIEH, Burgos, Spain), Rhawn Denniston (Department of Geology, Cornell College, Mount Vernon, IA  
304 52314, USA), Virgil Dragusin (Emil Racovita Institute of Speleology, 010986, Strada Frumoasă 31,  
305 Bucharest, Romania), Russell Drysdale (School of Geography, University of Melbourne, Melbourne,  
306 Australia), Oana Dumitru (Karst Research Group, School of Geosciences, University of South Florida, 4202  
307 E. Fowler Ave., NES 107, Tampa, FL 33620, USA), Amy Frappier (Department of Geosciences, Skidmore  
308 College, Saratoga Springs, New York, USA), Naveen Gandhi (Indian Institute of Tropical Meteorology, Dr.  
309 Homi Bhabha Road, Pashan, Pune-411008, India), Pawan Gautam (Centre for Earth, Ocean and



310 Atmospheric Sciences, University of Hyderabad, India; now at Geological Survey of India, Northern Region,  
311 India), Li Hanying (Institute of Global Environmental Change, Xi'an Jiaotong University, China), Ilaria Isola  
312 (Istituto Nazionale di Geofisica e Vulcanologia, Pisa, Italy), Xiuyang Jiang (College of Geography Science,  
313 Fujian Normal University, Fuzhou 350007, China), Zhao Jingyao (Institute of Global Environmental Change,  
314 Xi'an Jiaotong University, China), Kathleen Johnson (Dept. of Earth System Science, University of  
315 California, Irvine, 3200 Croul Hall, Irvine, CA 92697 USA), Vanessa Johnston (Research Centre of Slovenian  
316 Academy of Sciences and Arts ZRC SAZU, Novi trg 2, Ljubljana, Slovenia), Gayatri Kathayat (Institute of  
317 Global Environmental Change, Xi'an Jiaotong University, China), Jennifer Klose (Institut für  
318 Geowissenschaften, Johannes Gutenberg-Universität Mainz, Germany), Claire Krause (Geoscience  
319 Australia, Canberra, Australian Capital Territory, 2601, Australia), Matthew Lachniet (Department of  
320 Geoscience, University of Nevada Las Vegas, Las Vegas, NV 89154), Amzad Laskar (Geosciences Division,  
321 Physical Research Laboratory, Navrangpura, Ahmedabad 380009, India), Stein-Erik Lauritzen (University  
322 of Bergen, Earth science, Norway), Nina Loncar (University of Zadar, Department of Geography, 23000,  
323 Ulica Mihovila Pavlinovića, Zadar, Croatia), Gina Moseley (Institute of Geology, University of Innsbruck,  
324 Innrain 52, 6020 Innsbruck, Austria), Allu C Narayana (Centre for Earth, Ocean and Atmospheric Sciences,  
325 University of Hyderabad, India), Bogdan P. Onac (University of South Florida, School of Geosciences, 4202  
326 E Fowler Ave, Tampa, FL 33620, USA, Emil Racovita Institute of Speleology, Cluj-Napoca, Romania), Jacek  
327 Pawlak (Institute of Geological Sciences, Polish Academy of Sciences, 00-818, Twarda 51/55, Warsaw,  
328 Poland), Christopher Bronk Ramsey (Research Laboratory for Archaeology and the History of Art, Oxford  
329 University, Oxford, UK), Isabel Rivera-Collazo (Department of Anthropology and the Scripps Institution of  
330 Oceanography, UC San Diego, USA), Carlos Rossi (Dept. Petrología y Geoquímica, Facultad de Ciencias  
331 Geológicas, Universidad Complutense, Madrid, Spain), Peter J. Rowe (School of Environmental Sciences,  
332 University of East Anglia, NR4 7TJ, Norwich Research Park, Norwich, UK), Nicolás M. Strikis (Department  
333 of Geochemistry, Universidade Federal Fluminense, Niterói, Brazil), Liangcheng Tan (State Key Laboratory  
334 of Loess and Quaternary Geology, Institute of Earth Environment, Chinese Academy of Sciences, Xi'an  
335 710075, China), Sophie Verheyden (Politique scientifique fédérale belge BELSPO, Bvd. Simon Bolivar  
336 30,1000 Brussels), Hubert Vonhof (Max Planck Institute for Chemistry, Mainz, Germany), Michael Weber  
337 (Johannes Gutenberg-Universität Mainz, Germany), Kathleen Wendt (Geo- und  
338 Atmosphärenwissenschaften, Universität Innsbruck, Austria), Paul Wilcox (Institute of Geology, University  
339 of Innsbruck, Austria), Amos Winter (Dept. of Earth and Environmental Systems, Indiana State University,  
340 USA), Jiangying Wu (School of Geography, Nanjing Normal University, Nanjing, China), Peter Wynn  
341 (Lancaster Environment Centre, University of Lancaster, Lancaster, LA1 4YQ UK), Madhusudan G. Yadava  
342 (Geosciences Division, Physical Research Laboratory, Navrangpura, Ahmedabad 380009, India).



343 **Competing Interests:**

344 The authors declare no competing interests.

345 **Funding:**

346 SISAL (Speleothem Isotopes Synthesis and Analysis) is a working group of the Past Global Changes (PAGES)  
347 programme. We thank PAGES for their support for this activity. The design and creation of v2 of the  
348 database was supported by funding to SPH from the ERC-funded project GC2.0 (Global Change 2.0:  
349 Unlocking the past for a clearer future, grant number 694481) and the Geological Survey Ireland Short Call  
350 2017 (Developing a toolkit for model evaluation using speleothem isotope data, grant number 2017-SC-  
351 056) award to LCB. SPH and LCB acknowledge additional support from the ERC-funded project GC2.0 and  
352 from the JPI-Belmont project “PALaeo-Constraints on Monsoon Evolution and Dynamics (PACMEDY)”  
353 through the UK Natural Environmental Research Council (NERC). KR and DS acknowledge support by the  
354 Deutsche Forschungsgemeinschaft (DFG, codes RE3994/2-1 and SCHO 1274/11-1).

355 **Acknowledgements**

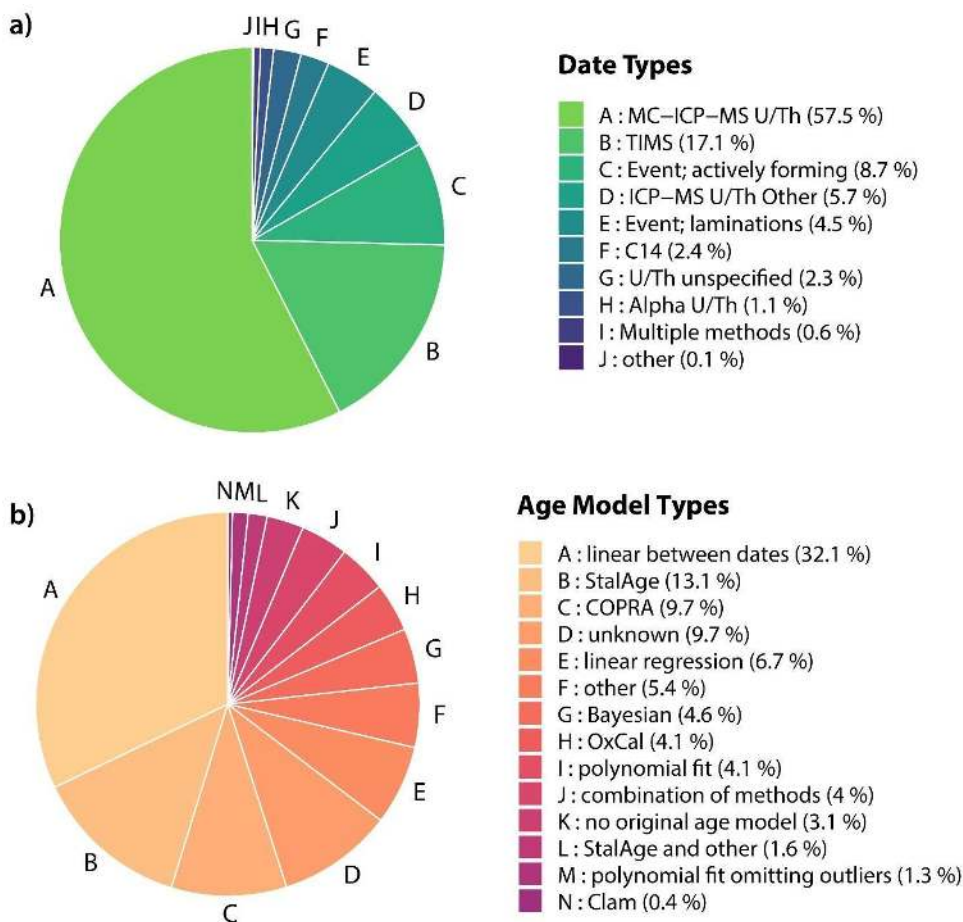
356 SISAL (Speleothem Isotopes Synthesis and Analysis) is a working group of the Past Global Changes (PAGES)  
357 programme. We thank PAGES for their support for this activity. We thank SISAL members who  
358 contributed their published data to the database and provided additional information when necessary.  
359 We thank all experts who engaged in the age-depth model evaluation. The authors would like to  
360 acknowledge Avner Ayalon, Jordi López, Bahadur Singh Kotlia, Dennis Rupprecht.

361



362 **List of Figures and Tables**

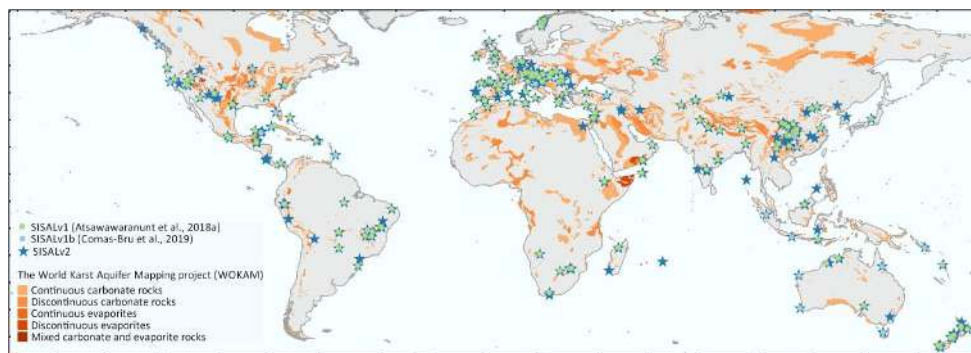
363 **Figure 1:** Summary of the dating information on which the original age-depth models are based  
 364 (a) and the original age-depth model types (b) present in SISALv2.  
 365



366  
 367  
 368

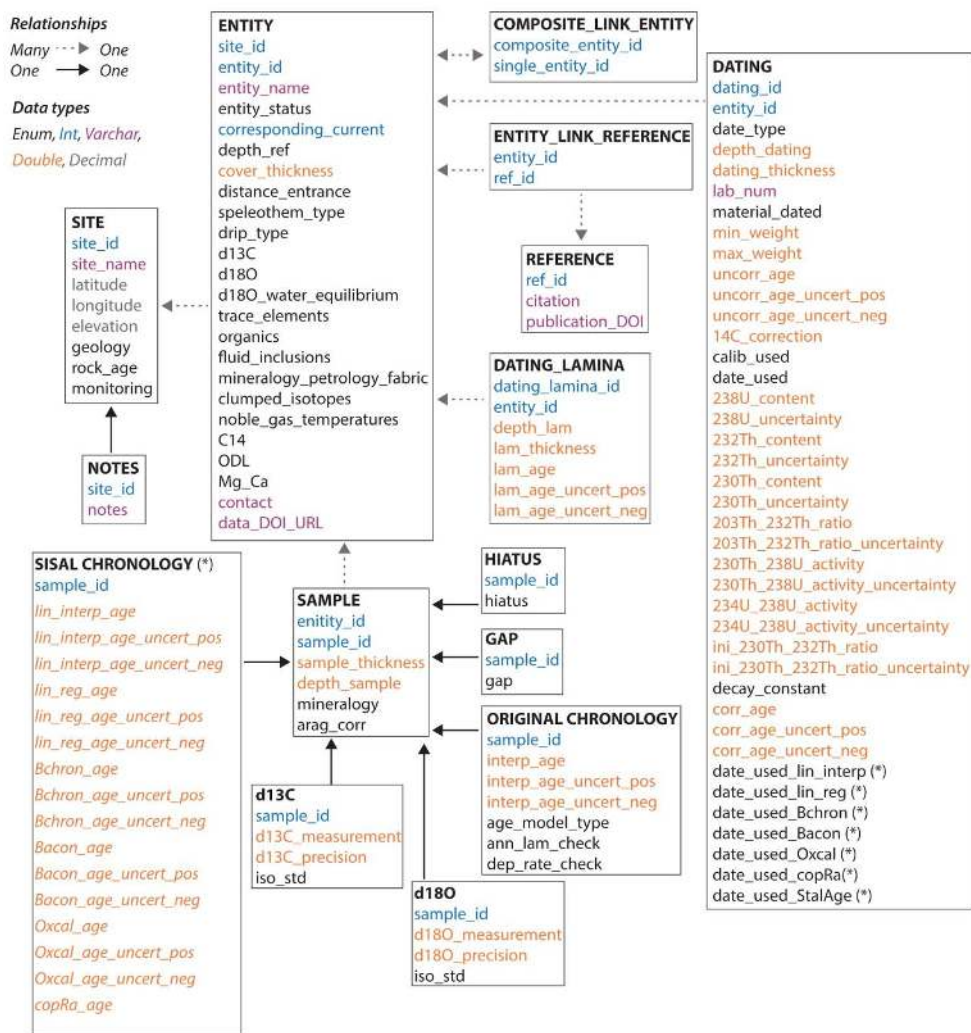


369 **Figure 2:** Cave sites included in the version 1, 1b and 2 of the SISAL database on the Global Karst  
370 Aquifer Map (WOKAM project; Chen et al., 2017: [https://www.un-igrac.org/resource/world-  
karst-aquifer-map-wokam](https://www.un-igrac.org/resource/world-<br/>371 karst-aquifer-map-wokam)).





374 **Figure 3:** The structure of the SISAL database version 2. Fields and table marked with (\*) refer to  
 375 new information added to SISALv1b; see tables 1 and 2 for details. The colours refer to the format  
 376 of that field: Enum, Int, Varchar, Double or Decimal. More information on the list of pre-defined  
 377 menus can be found in Atsawawaranunt et al. (2018a).  
 378

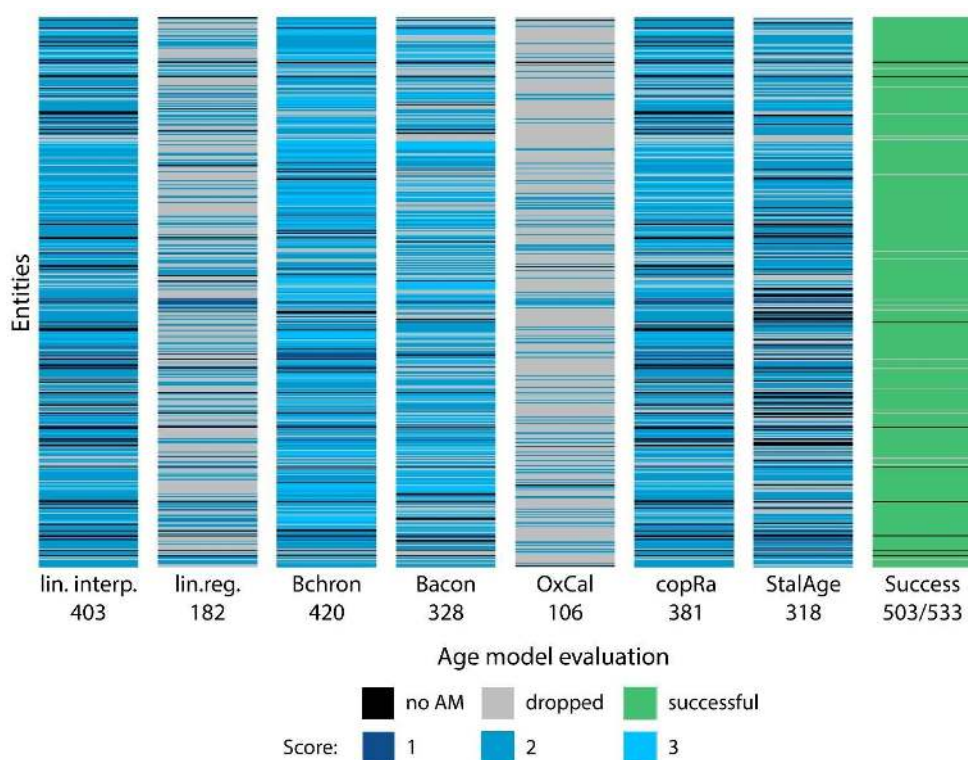


379  
 380





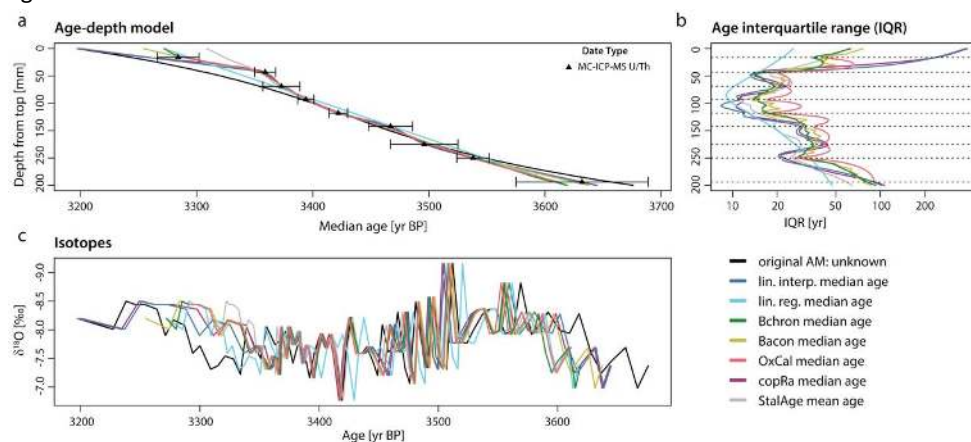
381 **Figure 4:** Visual summary of quality control of the automated SISAL chronology construction.  
382 The evaluation of the age-depth models for each method (x-axis) is given for each entity (y-axis)  
383 that was considered for the construction (n=533). Black lines mark age-depth models that could  
384 not be computed. Age-depth models dropped in the automated or expert evaluation are  
385 marked by grey lines. Age-depth models retained in SISALv2 are scored from 1 (only one  
386 criterion satisfied) to 3 (all criteria satisfied) in shades of blue. For 504 records alternative age-  
387 depth models with uncertainties are provided (green lines) in the “success” column.



388



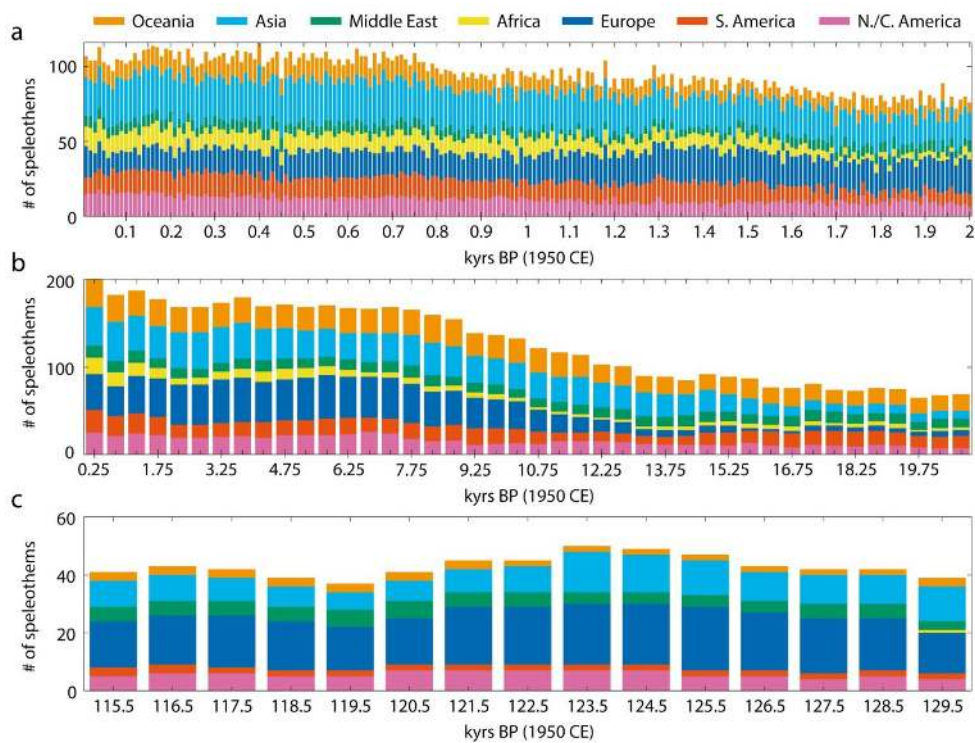
389 **Figure 5:** Illustration of the impact of the age model choice on reconstructed speleothem  
390 chronology illustrated by the KNI-51-H speleothem record (entity\_id 342; Denniston et al.,  
391 2013b). Panel (a) shows the median and mean age estimates for each downcore sample from  
392 the different age models; (b) shows the interquartile range (IQR) of the ages. Horizontal dashed  
393 lines show the depths of the measured dates; (c) shows the isotopic record using the different  
394 age models.



395  
396



397 **Figure 6:** Global and regional temporal coverage of entities in the SISALv2. (a) last 2,000 years  
398 with a bin size of 10 years; (b) last 21,000 years with a bin size of 500 years; (c) the period between  
399 115,000 and 130,000 years BP with a bin size of 1,000 yrs. BP refers to “Before Present” where  
400 present is 1950 CE. Regions defined as in Table 7.



401  
402



403 **Table 1:** Details of the `sisal_chronology` table. All ages in SISAL are reported as years BP (Before  
 404 Present) where present is 1950 CE.  
 405

Field label	Description	Format	Constraints
<code>sample_id</code>	Refers to the unique identifier for the sample (as given in the sample table)	Numeric	Positive integer
<code>lin_interp_age</code>	Age of the sample in years calculated with linear interpolation between dates	Numeric	None
<code>lin_interp_age_uncert_pos</code>	Positive 2-sigma uncertainty of the age of the sample in years calculated with linear interpolation between dates	Numeric	Positive decimal
<code>lin_interp_age_uncert_neg</code>	Negative 2-sigma uncertainty of the age of the sample in years calculated with linear interpolation between dates	Numeric	Positive decimal
<code>lin_reg_age</code>	Age of the sample in years calculated with linear regression	Numeric	None
<code>lin_reg_age_uncert_pos</code>	Positive 2-sigma uncertainty of the age of the sample in years calculated with linear regression	Numeric	Positive decimal
<code>lin_reg_age_uncert_neg</code>	Negative 2-sigma uncertainty of the age of the sample in years calculated with linear regression	Numeric	Positive decimal
<code>Bchron_age</code>	Age of the sample in years calculated with Bchron	Numeric	None
<code>Bchron_age_uncert_pos</code>	Positive 2-sigma uncertainty of the age of the sample in years calculated with Bchron	Numeric	Positive decimal
<code>Bchron_age_uncert_neg</code>	Negative 2-sigma uncertainty of the age of the sample in years calculated with Bchron	Numeric	Positive decimal
<code>Bacon_age</code>	Age of the sample in years calculated with Bacon	Numeric	None
<code>Bacon_age_uncert_pos</code>	Positive 2-sigma uncertainty of the age of the sample in years calculated with Bacon	Numeric	Positive decimal
<code>Bacon_age_uncert_neg</code>	Negative 2-sigma uncertainty of the age of the sample in years calculated with Bacon	Numeric	Positive decimal
<code>OxCal_age</code>	Age of the sample in years calculated with OxCal	Numeric	None
<code>OxCal_age_uncert_pos</code>	Positive 2-sigma uncertainty of the age of the sample in years calculated with OxCal	Numeric	Positive decimal
<code>OxCal_age_uncert_neg</code>	Negative 2-sigma uncertainty of the age of the sample in years calculated with OxCal	Numeric	Positive decimal
<code>copRa_age</code>	Age of the sample in years calculated with copRa	Numeric	None
<code>copRa_age_uncert_pos</code>	Positive 2-sigma uncertainty of the age of the sample in years calculated with copRa	Numeric	Positive decimal



<i>copRa_age_uncert_neg</i>	Negative 2-sigma uncertainty of the age of the sample in years calculated with copRa	Numeric	Positive decimal
<i>Stalage_age</i>	Age of the sample in years calculated with StalAge	Numeric	None
<i>Stalage_age_uncert_pos</i>	Positive 2-sigma uncertainty of the age of the sample in years calculated with StalAge	Numeric	Positive decimal
<i>Stalage_age_uncert_neg</i>	Negative 2-sigma uncertainty of the age of the sample in years calculated with StalAge	Numeric	Positive decimal

406

407 **Table 2:** Changes made to the Dating table to accommodate the new age models. These  
 408 changes are marked with (\*) in Figure 2.

409

Action	Field label	Description	Format	Constraints
Field added	<i>date_used_lin_age</i>	Indication whether that date was used to construct the linear age model	Text	Selected from pre-defined list: "yes", "no".
Field added	<i>date_used_lin_reg</i>	Indication whether that date was used to construct the age model based on linear regression	Text	Selected from pre-defined list: "yes", "no".
Field added	<i>date_used_Bchron</i>	Indication whether that date was used to construct the age model based on Bchron	Text	Selected from pre-defined list: "yes", "no".
Field added	<i>date_used_Bacon</i>	Indication whether that date was used to construct the age model based on Bacon	Text	Selected from pre-defined list: "yes", "no".
Field added	<i>date_used_OxCal</i>	Indication whether that date was used to construct the age model based on OxCal	Text	Selected from pre-defined list: "yes", "no".
Field added	<i>date_used_copRa</i>	Indication whether that date was used to construct the copRa_based age model	Text	Selected from pre-defined list: "yes", "no".
Field added	<i>date_used_StalAge</i>	Indication whether that date was used to construct the age model based on StalAge	Text	Selected from pre-defined list: "yes", "no".

410

411



412 **Table 3:** Changes made to tables other than the `sisal_chronology` since the publication of SISALv1  
 413 (Atsawawaranunt et al., 2018a; Atsawawaranunt et al., 2018b).

Table name	Action	Field label	Reason	Format	Constraints
Dating	Removed "sampling gap" option	<code>date_type</code>	This option was never used	Text	Selected from pre-defined list
	"others" option changed to "other"	<code>decay_constant</code>	Correction of typo	Text	Selected from pre-defined list
	Added "other" option	<code>calib_used</code>	Option added to accommodate new entities	Text	Selected from pre-defined list
	Added "other" option	<code>date_type</code>	Option added to accommodate new entities	Text	Selected from pre-defined list
Sample	Added "other" option	<code>original_chronology</code>	Option added to accommodate new entities	Text	Selected from pre-defined list
	Added "other" option	<code>ann_lam_check</code>	Option added to accommodate new entities	Text	Selected from pre-defined list

414

415 **Table 4:** Summary of the modifications applied to records already in version 1 (Atsawawaranunt  
 416 et al., 2018b) and version 1b (Atsawawaranunt et al., 2019) of the SISAL database. Mistakes in  
 417 previous versions of the database were identified as outlined in the Supplementary material and  
 418 through analysing the data for the SISAL publications.

419

Modification	V1 to v1b	V1b to v2
<b>Site table</b>		
Number of new sites	37	82
Sites with new entities	11	32
Sites with altered site.site_name altered	3	15
Sites with changes in site.latitude	4	29
Sites with changes in site.longitude	6	32
Sites with changes in site.elevation	13	11
Sites with site.geology updated	7	6
Sites with site.rock_age info updated	3	8
Sites with site.monitoring info updated	0	13
<b>Entity table</b>		
Number of new entities	74	236
How many entities were added to pre-existing sites?	17	84
Entities with revised entity_name	2	25
Entities with updated entity.entity_status	1	10



Entities with altered entity.corresponding current	0	11
Entities with altered entity.depth_ref?	0	1
Entities with altered entity.cover_thickness	1	3
Entities with altered entity.distance_entrance	0	3
Entities with revised entity.speleothem_type	14	4
Entities with revised entity.drip_type	10	2
Entities with altered entity.d13C	1	0
Entities with altered entity.d18O	1	0
Entities with altered entity.d18O_water_equilibrium	4	6
Entities with altered entity.trace_elements	1	2
Entities with altered entity.organics	1	2
Entities with altered entity.fluid_inclusions	1	3
Entities with altered entity.mineralogy_petrology_fabric	1	2
Entities with altered entity.clumped_isotopes	1	3
Entities with altered entity.noble_gas_temperatures	1	2
Entities with altered entity.C14	1	2
Entities with altered entity.ODL	1	2
Entities with altered entity.Mg_Ca	1	2
Entities with altered entity.contact (mostly correction of typos)	7	32
Entities with altered entity.Data_DOI_URL (revision mostly to permanent links)	134	14
<b>Dating table</b>		
Entities with changes in the dating table	70	260
Addition of "Event: hiatus" to an entity	0	3
How many hiatuses had their depth changed?	2	7
Entities with the depths of "Event: start/end of laminations" changed.	0	5
Entities with altered dating.date_type	11	30
Entities with altered dating.depth_dating	14	45
Entities with altered dating.dating_thickness	14	37
Entities with altered dating.material_dated	5	62
Entities with altered dating.min_weight	13	56
Entities with altered dating.max_weight	19	36
Entities with altered dating.uncorr_age	18	48
Entities with altered dating.uncorr_age_uncert_pos	12	53
Entities with altered dating.uncorr_age_uncert_neg	12	41
Entities with altered dating.14C_correction	17	36
Entities with altered dating.calib_used	13	32
Entities with altered dating.date_used	4	51
Entities with altered dating.238U_content	11	45
Entities with altered dating.238U_uncertainty	16	28
Entities with altered dating.232Th_content	15	46
Entities with altered dating.232Th_uncertainty	14	50
Entities with altered dating.230Th_content	11	40
Entities with altered dating.230Th_uncertainty	15	38
Entities with altered dating.230Th_232Th_ratio	5	59
Entities with altered dating.230Th_232Th_ratio_uncertainty	14	48
Entities with altered dating.230Th_238U_activity	19	39



Entities with altered dating.230Th_238U_activity_uncertainty	17	44
Entities with altered dating.234U_238U_activity	12	51
Entities with altered dating.234U_238U_activity_uncertainty	11	48
Entities with altered dating.ini_230Th_232Th_ratio	15	59
Entities with altered dating.ini_230Th_232Th_ratio_uncertainty	8	60
Entities with altered dating.decay_constant	17	55
Entities with altered dating.corr_age	17	35
Entities with altered dating.corr_age_uncert_pos	13	46
Entities with altered dating.corr_age_uncert_neg	9	47
<b>Sample table</b>		
Altered sample.depth_sample	0	15
Altered sample.mineralogy	0	20
Altered sample.arag_corr	11	20
How many entities had their d18O time-series altered (i.e. changes in depth and/or isotope values as in duplicates)?	13	95
How many entities had their d13C time-series altered (i.e. changes in depth and/or isotope values as in duplicates)?	8	64
<b>Original chronology</b>		
Entities with altered original_chronology.interp_age	1	42
Entities with altered original_chronology.interp_age_uncert_pos	0	14
Entities with altered original_chronology.interp_age_uncert_neg	0	14
<b>References</b>		
How many entities had their references changed (changes/additions/removals)?	6	16
How many citations have a different pub_DOI?	2	16
<b>Notes</b>		
Sites with notes removed	7	5
Sites with notes added	32	68
Sites with notes modified	21	34

420  
 421  
 422  
 423  
 424

**Table 5:** Information on new speleothem records (entities) added to the SISAL\_v2 database from SISALv1b (Comas-Bru et al., 2019). There may be multiple entities from a single cave, here identified as the site. Latitude (Lat) and Longitude (Lon) are given in decimal degrees North and East respectively.

Site_id	Site_name	Lat (N)	Lon (E)	Region	Entity_id	Entity_name	Reference
2	Kesang cave	42.87	81.75	China	620	CNKS-2	Cai et al. (2017)
					621	CNKS-3	Cai et al. (2017)
					622	CNKS-7	Cai et al. (2017)
					623	CNKS-9	Cai et al. (2017)
6	Hulu cave	32.5	119.17	China	617	MSP	Cheng et al. (2006)
					618	MSX	Cheng et al. (2006)





					619	MSH	Cheng et al. (2006)
12	Mawmluh cave	25.2622	91.8817	India	476	ML.1	Kathayat et al. (2018)
					477	ML.2	Kathayat et al. (2018)
					495	KM-1	Huguet et al. (2018)
13	Ball Gown cave	-17.03	125	Australia	633	BGC-5	Denniston et al. (2013b); Denniston et al. (2017a)
					634	BGC-10	Denniston et al. (2013b); Denniston et al. (2017a)
					635	BGC-11_2017	Denniston et al. (2013b); Denniston et al. (2017a)
					636	BGC-16	Denniston et al. (2013b); Denniston et al. (2017a)
14	Lehman caves	39.01	-114.22	United States	641	CDR3	Steponaitis et al. (2015)
					642	WR11	Steponaitis et al. (2015)
15	Baschg cave	47.2501	9.6667	Austria	643	BA-5	Moseley et al. (2019)
					644	BA-7	Moseley et al. (2019)
23	Lapa grande cave	-14.37	-44.28	Brazil	614	LG12B	Stríkis et al. (2018)
					615	LG10	Stríkis et al. (2018)
					616	LG25	Stríkis et al. (2018)
24	Lapa sem fim cave	-16.1503	-44.6281	Brazil	603	LSF15	Stríkis et al. (2018)
					604	LSF3_2018	Stríkis et al. (2018)
					605	LSF13	Stríkis et al. (2018)
					606	LSF11	Stríkis et al. (2018)
					607	LSF9	Stríkis et al. (2018)



27	Tamboril cave	-16	-47	Brazil	594	TM6	Ward et al. (2019)
39	Dongge cave	25.2833	108.0833	China	475	DA_2009	Cheng et al. (2009)
54	Sahiya cave	30.6	77.8667	India	478	SAH-2	Kathayat et al. (2017)
					479	SAH-3	Kathayat et al. (2017)
					480	SAH-6	Kathayat et al. (2017)
65	Whiterock cave	4.15	114.86	Malaysia (Borneo)	685	WR12-01	Carolin et al. (2016)
					686	WR12-12	Carolin et al. (2016)
72	Ascunsa cave	45	22.6	Romania	582	POM1	Staubwasser et al. (2018)
82	Hollywood cave	-41.95	171.47	New Zealand	673	HW-1	Williams et al. (2005)
86	Modric cave	44.2568	15.5372	Croatia	631	MOD-27	Rudzka-Phillips et al. (2013)
					632	MOD-21	Rudzka et al. (2012)
105	Schneckenloch cave	47.4333	9.8667	Austria	663	SCH-6	Moseley et al. (2019)
113	Paixao cave	-	-	Brazil	611	PX5	Strikis et al. (2015)
		12.6182	41.0184		612	PX7_2018	Stríkis et al. (2018)
115	Hölloch im Mahdtal	47.3781	10.1506	Germany	664	HOL-19	Moseley et al. (2019)
117	Bunker cave	51.3675	7.6647	Germany	596	Bu2_2018	Weber et al. (2018)
128	Buckeye creek	37.98	-80.4	United States	681	BCC-9	Cheng et al. (2019)
					682	BCC-10_2019	Cheng et al. (2019)
					683	BCC-30	Cheng et al. (2019)
135	Grotte de Piste	33.95	-4.246	Morocco	464	GP5	Ait Brahim et al. (2018)
					591	GP2	Ait Brahim et al. (2018)
138	Moomi cave	12.55	54.2	Yemen (Socotra)	481	M1-2	Mangini, Cheng et al., unpublished; Burns et al. (2003) Burns et al. (2004)
140	Sanbao cave	31.667	110.4333	China	482	SB3	Wang et al. (2008)
					483	SB-10_2008	Wang et al. (2008)



					484	SB11	Wang et al. (2008)
					485	SB22	Wang et al. (2008)
					486	SB23	Wang et al. (2008)
					487	SB24	Wang et al. (2008)
					488	SB25-1	Wang et al. (2008)
					489	SB25-2	Wang et al. (2008)
					490	SB-26_2008	Wang et al. (2008)
					491	SB34	Wang et al. (2008)
					492	SB41	Wang et al. (2008)
					493	SB42	Wang et al. (2008)
					494	TF	Wang et al. (2008)
141	Sofular cave	41.4167	31.9333	Turkey	456	SO-2	Badertscher et al. (2011) Fleitmann et al. (2009); Göktürk et al. (2011)
					687	SO-4	Badertscher et al. (2011)
					688	SO-6	Badertscher et al. (2011)
					689	SO-14B	Badertscher et al. (2011)
145	Antro del Corchia	43.9833	10.2167	Italy	665	CC-1_2018	Tzedakis et al. (2018)
					666	CC-5_2018	Tzedakis et al. (2018)
					667	CC-7_2018	Tzedakis et al. (2018)
					668	CC-28_2018	Tzedakis et al. (2018)
					669	CC_stack	Tzedakis et al. (2018)
					670	CC27	Isola et al. (2019)
155	KNI-51	-15.3	128.62	Australia	637	KNI-51-1	Denniston et al. (2017a)
					638	KNI-51-8	Denniston et al. (2017a)
160	Soreq cave	31.7558	35.0226	Israel	690	Soreq-composite185	Bar-Matthews et al. (2003)



165	Ruakuri cave	-36.27	175.08	New Zealand	674	RK-A	Williams et al. (2010)
165	Ruakuri cave	-36.27	175.08	New Zealand	675	RK-B	Williams et al. (2010)
165	Ruakuri cave	-36.27	175.08	New Zealand	676	RK05-1	Whittaker (2008)
165	Ruakuri cave	-36.27	175.08	New Zealand	677	RK05-3	Whittaker (2008)
165	Ruakuri cave	-36.27	175.08	New Zealand	678	RK05-4	Whittaker (2008)
177	Santo Tomas cave	22.55	-83.84	Cuba	608	CM_2019	Warken et al. (2019)
					609	CMa	Warken et al. (2019)
					610	CMb	Warken et al. (2019)
179	Closani Cave	45.10	22.8	Romania	390	C09-2	Warken et al. (2018)
182	Kotumsar cave	19	82	India	590	KOT-I	Band et al. (2018)
192	El Condor cave	-5.93	-77.3	Peru	592	ELC-A	Cheng et al. (2013)
					593	ELC-B	Cheng et al. (2013)
198	Lianhua cave, Hunan	29.48	109.5333	China	496	LH-2	Zhang et al. (2013)
213	Tausoare cave	47.4333	24.5167	Romania	457	1152	Staubwasser et al. (2018)
214	Cave C126	-22.1	113.9	Australia	458	C126-117	Denniston et al. (2013a)
					459	C126-118	Denniston et al. (2013a)
215	Chaara cave	33.9558	-4.2461	Morocco	460	Cha2_2018	Ait Brahim et al. (2018)
					588	Cha2_2019	Ait Brahim et al. (2019)
					589	Cha1	Ait Brahim et al. (2019)
216	Dark cave	27.2	106.1667	China	461	D1	Jiang et al. (2013)
					462	D2	Jiang et al. (2013)
217	E'mei cave	29.5	115.5	China	463	EM1	Zhang et al. (2018b)
218	Nuanhe cave	41.3333	124.9167	China	465	NH6	Wu et al. (2012)
					466	NH33	Wu et al. (2012)
219	Shennong cave	28.71	117.26	China	467	SN17	Zhang et al. (2018a)
220	Baeg-nyong cave	37.27	128.58	South Korea	468	BN-1	Jo et al. (2017)



221	La Vierge cave	-19.7572	63.3703	Rodrigues	469	LAVI-4	Li et al. (2018)
222	Patate cave	-19.7583	63.3864	Rodrigues	470	PATA-1	Li et al. (2018)
223	Wanxiang cave	33.32	105	China	471	WX42B	Zhang et al. (2008)}
					679	WXSM-51	Johnson et al. (2006)
					680	WXSM-52	Johnson et al. (2006)
224	Xianglong cave	33	106.33	China	472	XL16	Tan et al. (2018a)
					473	XL2	Tan et al. (2018a)
					474	XL26	Tan et al. (2018a)
225	Chiflonkhakha cave	-18.1222	-65.7739	Bolivia	497	Boto 1	Apaestegui et al. (2018)
					498	Boto 3	Apaestegui et al. (2018)
					499	Boto 7	Apaestegui et al. (2018)
226	Cueva del Diamante	-5.73	-77.5	Peru	500	NAR-C	Cheng et al. (2013)
					501	NAR-C-D	Cheng et al. (2013)
					502	NAR-C-F	Cheng et al. (2013)
					503	NAR-D	Cheng et al. (2013)
					504	NAR-F	Cheng et al. (2013)
227	El Capitan cave	56.162	-133.319	United States	505	EC-16-5-F	Wilcox et al. (2019)
228	Bat cave	32.1	-104.26	United States	506	BC-11	Asmerom et al. (2013)
229	Actun Tunichil Muknal	17.1	-88.85	Belize	507	ATM-7	Frappier et al. (2002); Frappier et al. (2007); Jamieson et al. (2015)
230	Marota cave	-12.6227	-41.0216	Brazil	508	MAG	Stríkis et al. (2018)
231	Pacupahuain cave	-11.24	-75.82	Peru	509	P09PH2	Kanner et al. (2012)
232	Rio Secreto cave system	20.59	-87.13	Mexico	510	Itzamna	Medina-Elizalde et al., (2016); Medina-Elizalde et al. (2017)



233	Robinson cave	33	-107.7	United States	511	KR1	Polyak et al. (2017)
234	Santana cave	-24.5308	-48.7267	Brazil	512	St8-a	Cruz et al. (2006)
					513	St8-b	Cruz et al. (2006)
235	Cueva del Tigre Perdido	-5.9406	-77.3081	Peru	514	NC-A	van Breukelen et al. (2008)
					515	NC-B	van Breukelen et al. (2008)
236	Toca da Boa Vista	-10.1602	-40.8605	Brazil	516	TBV40	Wendt et al. (2019)
					517	TBV63	Wendt et al. (2019)
237	Umajalanta cave	-18.12	-65.77	Bolivia	518	Boto 10	Apaestegui et al. (2018)
238	Akalagavi cave	14.9833	74.5167	India	519	MGY	Yadava et al. (2004)
239	Baluk cave	42.433	84.733	China	520	BLK12B	Liu et al. (2019)
240	Baratang cave	12.0833	92.75	India	521	AN4	Laskar et al. (2013)
					522	AN8	Laskar et al. (2013)
241	Gempa bumi cave	-5	120	Indonesia (Sulawesi)	523	GB09-03	Krause et al. (2019)
					524	GB11-09	Krause et al. (2019)
242	Haozhu cave	30.6833	109.9833	China	525	HZZ-11	Zhang et al. (2016)
					526	HZZ-27	Zhang et al. (2016)
243	Kailash cave	18.8445	81.9915	India	527	KG-6	Gautam et al. (2019)
244	Lianhua cave, Shanxi	38.1667	113.7167	China	528	LH1	Dong et al. (2018)
					529	LH4	Dong et al. (2018)
					530	LH5	Dong et al. (2018)
					531	LH6	Dong et al. (2018)
					532	LH9	Dong et al. (2018)
					533	LH30	Dong et al. (2018)
245	Nakarallu cave	14.52	77.99	India	534	NK-1305	Sinha et al. (2018)
246	Palawan cave	10.2	118.9	Malaysia (Northern Borneo)	535	SR02	Partin et al. (2015)
247	Shalaih cave	35.1469	45.2958	Iraq	536	SHC-01	Marsh et al. (2018); Amin Al-



							Manmi et al. (2019)
					537	SHC-02	Marsh et al. (2018); Amin Al-Manmi et al. (2019)
248	Shenqi cave	28.333	103.1	China	538	SQ1	Tan et al. (2018b)
					539	SQ7	Tan et al. (2018b)
249	Shigao cave	28.183	107.167	China	540	SG1	Jiang et al. (2012)
					541	SG2	Jiang et al. (2012)
250	Wuya cave	33.82	105.43	China	542	WY27	Tan et al. (2015)
					543	WY33	Tan et al. (2015)
251	Zhenzhu cave	38.25	113.7	China	544	ZZ12	Yin et al. (2017)
252	Andriamanilok e	- 24.051	43.7569	Madagascar	545	AD4	Scroxtton et al. (2019)
253	Hoq cave	12.5866	54.3543	Yemen (Socotra)	546	Hq-1	Van Rempelberg h et al. (2013)
					547	STM1	Van Rempelberg h et al. (2013)
					548	STM6	Van Rempelberg h et al. (2013)
254	PP29	- 34.2078	22.0876	South Africa	549	46745	Braun et al. (2019b)
					550	46746-a	Braun et al. (2019b)
					551	46747	Braun et al. (2019b)
					552	138862.1	Braun et al. (2019b)
					553	138862.2a	Braun et al. (2019b)
					554	142828	Braun et al. (2019b)
					555	46746-b	Braun et al. (2019b)
					556	138862.2b	Braun et al. (2019b)
255	Mitoho	- 24.0477	43.7533	Madagascar	557	MT1	Scroxtton et al. (2019)



256	Lithophagus cave	46.828	22.6	Romania	558	LFG-2	Lauritzen and Onac (1999)
257	Akcakale cave	40.4498	39.5365	Turkey	559	2p	Jex et al. (2010); Jex et al. (2011); Jex et al. (2013)
258	B7 cave	49	7	Germany	560	STAL-B7-7	Niggemann et al. (2003b)
259	Cobre cave	42.98	-4.37	Spain	561	PA-8	Osete et al. (2012); Rossi et al. (2014)
260	Crovassa Azzurra	39.28	8.48	Italy	562	CA	Columbu et al. (2019)
261	El Soplao cave	43.2962	-4.3937	Spain	563	SIR-1	Rossi et al. (2018)
262	Bleißberg cave	50.4244	11.0203	Germany	564	BB-1	Breitenbach et al. (2019)
					565	BB-3	Breitenbach et al. (2019)
263	Orlova Chuka cave	43.5937	25.9597	Bulgaria	566	ocz-6	Pawlak et al. (2019)
264	Strašna peć cave	44.0049	15.0388	Croatia	567	SPD-1	Lončar et al. (2019)
					568	SPD-2	Lončar et al. (2019)
265	Coves de Campanet	39.7937	2.9683	Spain	569	CAM-1	Dumitru et al. (2018)
266	Cueva Victoria	37.6322	-0.8215	Spain	570	Vic-III-4	Budsky et al. (2019)
267	Gruta do Casal da Lebre	39.3	-9.2667	Portugal	571	GCL6	Denniston et al. (2017b)
268	Pere Noel cave	50	5.2	Belgium	572	PN-95-5	Verheyden et al. (2000); Verheyden et al. (2014)
269	Gejkar cave	35.8	45.1645	Iraq	573	Gej-1	Flohr et al. (2017)
270	Gol-E-Zard cave	35.84	52	Iran	574	GZ14-1	Carolin et al. (2019)
271	Jersey cave	-35.72	148.49	Australia	575	YB-F1	Webb et al. (2014)
272	Metro cave	-41.93	171.47	New Zealand	576	M-1	Logan (2011)
273	Crystal cave	36.59	-118.82	United States	577	CRC-3	McCabe-Glynn et al. (2013)
274	Terciopelo cave	10.17	-85.33	Costa Rica	578	CT-1	Lachniet et al. (2009)
					579	CT-5	Lachniet et al. (2009)





					580	CT-6	Lachniet et al. (2009)
					581	CT-7	Lachniet et al. (2009)
275	Buraca Gloriosa	39.5333	-8.7833	Portugal	583	BG41	Denniston et al. (2017b)
					584	BG66	Denniston et al. (2017b)
					585	BG67	Denniston et al. (2017b)
					586	BG611	Denniston et al. (2017b)
					587	BG6LR	Denniston et al. (2017b)
276	Béke cave	48.4833	20.5167	Hungary	595	BNT-2	Demény et al. (2019)
							Czuppon et al. (2018)
277	Huagapo cave	-11.27	-75.79	Peru	597	P00-H2	Kanner et al. (2013)
					598	P00-H1	Kanner et al. (2013)
					599	P09-H1b	Burns et al. (2019)
					600	P10-H5	Burns et al. (2019)
					601	P10-H2	Burns et al. (2019)
					602	PeruMIS6Composi te	Burns et al. (2019)
278	Pink Panther cave	32	-105.2	United States	613	PP1	Asmerom et al. (2007)
279	Staircase cave	-34.2071	22.0899	South Africa	624	46322	Braun et al. (2019b)
					625	46330-a	Braun et al. (2019b)
					626	46861	Braun et al. (2019b)
					627	50100	Braun et al. (2019b)
					628	142819	Braun et al. (2019b)
					629	142820	Braun et al. (2019b)
					630	46330-b	Braun et al. (2019b)
280	Atta cave	51.1	7.9	Germany	639	AH-1	Niggemann et al. (2003a)
281	Venado cave	10.55	-84.77	Costa Rica	640	V1	Lachniet et al. (2004)



282	Wadi Sannur cave	28.6167	31.2833	Egypt	691	WS-5d	El-Shenawy et al. (2018)
283	Babylon cave	-41.95	171.47	New Zealand	645	BN-1	Williams et al. (2005)
					646	BN-2	Williams et al. (2005)
					647	BN-3	P. Williams et al., unpublished
284	Creighton's cave	-40.63	172.47	New Zealand	648	CN-1	Williams et al. (2005)
285	Disbelief cave	-38.82	177.52	New Zealand	649	Disbelief	Lorrey et al. (2008)
286	La Garma cave	43.4306	-3.6658	Spain	650	GAR-01_drill	Baldini et al. (2015); Baldini et al. (2019)
					651	GAR-01_laser_d18O	Baldini et al. (2015)
					652	GAR-01_laser_d13C	Baldini et al. (2015)
287	Twin Forks cave	-40.63	172.48	New Zealand	653	TF-2	Williams et al. (2005)
288	Wet Neck cave	-40.7	172.48	New Zealand	654	WN-4	Williams et al. (2005)
					655	WN-11	Williams et al. (2005)
289	Gassel Tropfsteinhöhle	47.8228	13.8428	Austria	656	GAS-12	Moseley et al. (2019)
					657	GAS-13	Moseley et al. (2019)
					658	GAS-22	Moseley et al. (2019)
					659	GAS-25	Moseley et al. (2019)
					660	GAS-27	Moseley et al. (2019)
					661	GAS-29	Moseley et al. (2019)
290	Grete-Ruth Shaft	47.5429	12.0272	Austria	662	HUN-14	Moseley et al. (2019)
292	Limnon cave	37.9605	22.1403	Greece	671	KTR-2	Peckover et al. (2019)
293	Tham Doun Mai	20.75	102.65	Laos	672	TM-17	Wang et al. (2019)
294	Palco cave	18.35	-66.5	Puerto Rico	684	PA-2b	Rivera-Collazo et al. (2015)
179	Closani Cave	45.10	22.8	Romania	390	C09-2	Warken et al. (2018)



426 **Table 6:** Percentage of entities uploaded to the different versions of the SISAL database with  
427 respect to the number of records identified by the SISAL working group as of November 2019.  
428 The number of identified records includes potentially superseded speleothem records. Regions  
429 are defined as: Oceania ( $-60^\circ < \text{Lat} < 0^\circ$ ;  $90^\circ < \text{Lon} < 180^\circ$ ); Asia ( $0^\circ < \text{Lat} < 60^\circ$ ;  $60^\circ < \text{Lon} < 130^\circ$ );  
430 Middle East ( $7.6^\circ < \text{Lat} < 50^\circ$ ;  $26^\circ < \text{Lon} < 59^\circ$ ); Africa ( $-45^\circ < \text{Lat} < 36.1^\circ$ ;  $-30^\circ < \text{Lon} < 60^\circ$ ; with  
431 records in the Middle East region removed); Europe ( $36.7^\circ < \text{Lat} < 75^\circ$ ;  $-30^\circ < \text{Lon} < 30^\circ$ ; plus  
432 Gibraltar and Siberian sites); South America (S. Am;  $-60^\circ < \text{Lat} < 8^\circ$ ;  $-150^\circ < \text{Lon} < -30^\circ$ ); North and  
433 Central America (N./C. Am;  $8.1^\circ < \text{Lat} < 60^\circ$ ;  $-150^\circ < \text{Lon} < -50^\circ$ )  
434

Region	Version 1		Version 1b		Version 2	
	Entities	Sites	Entities	Sites	Entities	Sites
Oceania	47.7	36.7	56.8	51.0	80.2	69.4
Asia	36.2	28.8	41.1	33.3	64.8	48.5
Middle East	21.2	31.1	28.8	35.6	42.3	48.9
Africa	63.2	62.5	63.2	62.5	73.7	87.5
Europe	48.0	51.9	54.6	58.7	75.3	77.9
S. Am	30.6	39.5	40.8	50.0	77.6	73.7
N./C. Am	35.7	36.7	51.8	56.7	70.5	73.3

435



## 436 References

- 437 Ait Brahim, Y., Wassenburg, J. A., Cruz, F. W., Sifeddine, A., Scholz, D., Bouchaou, L., Dassie, E. P., Jochum,  
438 K. P., Edwards, R. L., and Cheng, H.: Multi-decadal to centennial hydro-climate variability and linkage to  
439 solar forcing in the Western Mediterranean during the last 1000 years, *Scientific Reports*, 8, 174466,  
440 10.1038/s41598-018-35498-x, 2018.
- 441 Ait Brahim, Y., Wassenburg, J. A., Sha, L., Cruz, F. W., Deininger, M., Sifeddine, A., Bouchaou, L., Spötl, C.,  
442 Edwards, R. L., and Cheng, H.: North Atlantic Ice-Rafting, Ocean and Atmospheric Circulation During the  
443 Holocene: Insights From Western Mediterranean Speleothems, *Geophysical Research Letters*, 46,  
444 2019GL082405-082019GL082405, 10.1029/2019GL082405, 2019.
- 445 Amin Al-Manmi, D. A. M., Ismaeel, S. B., and Altaweel, M.: Reconstruction of palaeoclimate in Shalaih Cave,  
446 SE of Sangaw, Kurdistan Province of Iraq, *Palaeogeography, Palaeoclimatology, Palaeoecology*, 524, 262-  
447 272, 10.1016/j.PALAEO.2019.03.044, 2019.
- 448 Apaestegui, J., Cruz, F. W., Vuille, M., Fohlmeister, J., Espinoza, J. C., Sifeddine, A., Strikis, N., Guyot, J. L.,  
449 Ventura, R., Cheng, H., and Edwards, R. L.: Precipitation changes over the eastern Bolivian Andes inferred  
450 from speleothem ( $\delta$  O-18) records for the last 1400 years, *Earth and Planetary Science Letters*, 494,  
451 124-134, 10.1016/j.epsl.2018.04.048, 2018.
- 452 Asmerom, Y., Polyak, V., Burns, S., and Rasmussen, J.: Solar forcing of Holocene climate: New insights  
453 from a speleothem record, southwestern United States, *Geology*, 35, 1-4, 10.1130/G22865A.1, 2007.
- 454 Asmerom, Y., Polyak, V. J., Rasmussen, J. B. T., Burns, S. J., and Lachniet, M.: Multidecadal to multicentury  
455 scale collapses of Northern Hemisphere monsoons over the past millennium, *Proceedings of the National  
456 Academy of Sciences of the United States of America*, 110, 9651-9656, 10.1073/pnas.1214870110, 2013.
- 457 Atsawawaranunt, K., Comas-Bru, L., Amirnezhad Mozhdehi, S., Deininger, M., Harrison, S. P., Baker, A.,  
458 Boyd, M., Kaushal, N., Ahmad, S. M., Ait Brahim, Y., Arienzo, M., Bajo, P., Braun, K., Burstyn, Y., Chawchai,  
459 S., Duan, W., Hatvani, I. G., Hu, J., Kern, Z., Labuhn, I., Lachniet, M., Lechleitner, F. A., Lorrey, A., Pérez-  
460 Mejias, C., Pickering, R., Scroxton, N., and SISAL Working Group members, S. W. G.: The SISAL database: a  
461 global resource to document oxygen and carbon isotope records from speleothems, *Earth System Science  
462 Data*, 10, 1687-1713, 10.5194/essd-10-1687-2018, 2018a.
- 463 Atsawawaranunt, K., Harrison, S. and Comas-Bru, L.: SISAL (Speleothem Isotopes Synthesis and Analysis  
464 Working Group) database Version 1.0. University of Reading. Dataset.: 10.17864/1947.147 2018b.
- 465 Atsawawaranunt, K., Harrison, S. and Comas-Bru, L.: SISAL (Speleothem Isotopes Synthesis and Analysis  
466 Working Group) database Version 1b. University of Reading. Dataset.: 10.17864/1947.189, 2019.
- 467 Badertscher, S., Fleitmann, D., Cheng, H., Edwards, R. L., Göktürk, O. M., Zumbühl, A., Leuenberger, M.,  
468 and Tüysüz, O.: Pleistocene water intrusions from the Mediterranean and Caspian seas into the Black Sea,  
469 *Nature Geoscience*, 4, 236-239, 10.1038/ngeo1106, 2011.
- 470 Baldini, L. M., McDermott, F., Baldini, J. U. L., Arias, P., Cueto, M., Fairchild, I. J., Hoffmann, D. L., Matthey,  
471 D. P., Muller, W., Nita, D. C., Ontanon, R., Garcia-Monco, C., and Richards, D. A.: Regional temperature,  
472 atmospheric circulation, and sea-ice variability within the Younger Dryas Event constrained using a  
473 speleothem from northern Iberia, *Earth and Planetary Science Letters*, 419, 101-110,  
474 10.1016/j.epsl.2015.03.015, 2015.
- 475 Baldini, L. M., Baldini, J. U. L., McDermott, F., Arias, P., Cueto, M., Fairchild, I. J., Hoffmann, D. L., Matthey,  
476 D. P., Müller, W., Nita, D. C., Ontañón, R., García-Moncó, C., and Richards, D. A.: North Iberian temperature



- 477 and rainfall seasonality over the Younger Dryas and Holocene, *Quaternary Science Reviews*, 226, 105998,  
478 10.1016/j.quascirev.2019.105998, 2019.
- 479 Band, S., Yadava, M. G., Lone, M. A., Shen, C. C., Sree, K., and Ramesh, R.: High-resolution mid-Holocene  
480 Indian Summer Monsoon recorded in a stalagmite from the Kotumsar Cave, Central India, *Quaternary*  
481 *International*, 479, 19-24, 10.1016/j.quaint.2018.01.026, 2018.
- 482 Bar-Matthews, M., Ayalon, A., Gilmour, M., Matthews, A., and Hawkesworth, C. J.: Sea–land oxygen  
483 isotopic relationships from planktonic foraminifera and speleothems in the Eastern Mediterranean region  
484 and their implication for paleorainfall during interglacial intervals, *Geochimica et Cosmochimica Acta*, 67,  
485 3181-3199, 10.1016/S0016-7037(02)01031-1, 2003.
- 486 Blaauw, M.: Methods and code for ‘classical’ age-modelling of radiocarbon sequences, *Quaternary*  
487 *Geochronology*, 5, 512-518, 10.1016/j.quageo.2010.01.002, 2010.
- 488 Blaauw, M., and Christen, J. A.: Flexible Paleoclimate Age-Depth Models Using an Autoregressive Gamma  
489 Process, *Bayesian Analysis*, 6, 457-474, 10.1214/11-ba618, 2011.
- 490 Braun, K., Nehme, C., Pickering, R., Rogerson, M., and Scropton, N.: A Window into Africa’s Past  
491 Hydroclimates: The SISAL\_v1 Database Contribution, *Quaternary*, 2, 10.3390/quat2010004, 2019a.
- 492 Braun, K., Bar-Matthews, M., Matthews, A., Ayalon, A., Cowling, R. M., Karkanis, P., Fisher, E. C., Dyez, K.,  
493 Zilberman, T., and Marean, C. W.: Late Pleistocene records of speleothem stable isotopic compositions  
494 from Pinnacle Point on the South African south coast, *Quaternary Research*, 91, 265-288,  
495 10.1017/qua.2018.61, 2019b.
- 496 Breitenbach, S. F. M., Rehfeld, K., Goswami, B., Baldini, J. U. L., Ridley, H. E., Kennett, D. J., Prufer, K. M.,  
497 Aquino, V. V., Asmerom, Y., Polyak, V. J., Cheng, H., Kurths, J., and Marwan, N.: COConstructing Proxy Records  
498 from Age models (COPRA), *Climate of the Past*, 8, 1765-1779, 10.5194/cp-8-1765-2012, 2012.
- 499 Breitenbach, S. F. M., Plessen, B., Waltgenbach, S., Tjallingii, R., Leonhardt, J., Jochum, K. P., Meyer, H.,  
500 Goswami, B., Marwan, N., and Scholz, D.: Holocene interaction of maritime and continental climate in  
501 Central Europe: New speleothem evidence from Central Germany, *Global and Planetary Change*, 176, 144-  
502 161, 10.1016/J.GLOPLACHA.2019.03.007, 2019.
- 503 Bronk Ramsey, C.: Deposition models for chronological records, *Quaternary Science Reviews*, 27, 42-60,  
504 2008.
- 505 Bronk Ramsey, C.: Bayesian analysis of radiocarbon dates, *Radiocarbon*, 51, 337-360, 2009.
- 506 Bronk Ramsey, C., and Lee, S.: Recent and planned developments of the program OxCal, *Radiocarbon*, 55,  
507 720-730, 2013.
- 508 Budsky, A., Scholz, D., Wassenburg, J. A., Mertz-Kraus, R., Spötl, C., Riechelmann, D. F. C., Gibert, L.,  
509 Jochum, K. P., and Andrae, M. O.: Speleothem  $\delta^{13}C$  record suggests enhanced spring/summer drought  
510 in south-eastern Spain between 9.7 and 7.8 ka – A circum-Western Mediterranean anomaly?, *The*  
511 *Holocene*, 29, 1113-1133, 10.1177/0959683619838021, 2019.
- 512 Burns, S. J., Fleitmann, D., Matter, A., Kramers, J., and Al-Subbary, A. A.: Indian Ocean Climate and an  
513 Absolute Chronology over Dansgaard/Oeschger Events 9 to 13, *Science*, 301, 1365-1367,  
514 10.1126/science.1086227, 2003.
- 515 Burns, S. J., Fleitmann, D., Matter, A., Kramers, J., and Al-Subbary, A. A.: Corrections and Clarifications,  
516 *Science*, 305, 1567a-1567a, 10.1126/science.305.5690.1567a, 2004.



- 517 Burns, S. J., Welsh, L. K., Scroxton, N., Cheng, H., and Edwards, R. L.: Millennial and orbital scale variability  
518 of the South American Monsoon during the penultimate glacial period, *Scientific Reports*, 9, 1234,  
519 10.1038/s41598-018-37854-3, 2019.
- 520 Burstyn, Y., Martrat, B., Lopez, F. J., Iriarte, E., Jacobson, J. M., Lone, A. M., and Deininger, M.: Speleothems  
521 from the Middle East: An Example of Water Limited Environments in the SISAL Database, *Quaternary*, 2,  
522 10.3390/quat2020016, 2019.
- 523 Cai, Y. J., Chiang, J. C. H., Breitenbach, S. F. M., Tan, L. C., Cheng, H., Edwards, R. L., and An, Z. S.: Holocene  
524 moisture changes in western China, Central Asia, inferred from stalagmites, *Quaternary Science Reviews*, 2,  
525 158, 15-28, 10.1016/j.quascirev.2016.12.014, 2017.
- 526 Carolin, S. A., Cobb, K. M., Lynch-Stieglitz, J., Moerman, J. W., Partin, J. W., Lejau, S., Malang, J., Clark, B.,  
527 Tuen, A. A., and Adkins, J. F.: Northern Borneo stalagmite records reveal West Pacific hydroclimate across  
528 MIS 5 and 6, *Earth and Planetary Science Letters*, 439, 182-193, 10.1016/j.epsl.2016.01.028, 2016.
- 529 Carolin, S. A., Walker, R. T., Day, C. C., Ersek, V., Sloan, R. A., Dee, M. W., Talebian, M., and Henderson, G.  
530 M.: Precise timing of abrupt increase in dust activity in the Middle East coincident with 4.2 ka social  
531 change, *Proceedings of the National Academy of Sciences*, 116, 67-72, 10.1073/PNAS.1808103115, 2019.
- 532 Chen, Z., Auler, A. S., Bakalowicz, M., Drew, D., Griger, F., Hartmann, J., Jiang, G., Moosdorf, N., Richts, A.,  
533 Stevanovic, Z., Veni, G., and Goldscheider, N.: The World Karst Aquifer Mapping project: concept, mapping  
534 procedure and map of Europe, *Hydrogeology Journal*, 25, 771-785, 10.1007/s10040-016-1519-3, 2017.
- 535 Cheng, H., Edwards, R. L., Wan, Y. J., Ko, X. G., Ming, Y. F., Kelly, M. J., Wang, X. F., Gallup, C. D., and Liu,  
536 W. G.: A penultimate glacial monsoon record from Hulu Cave and two-phase glacial terminations, *Geology*,  
537 34, 217-220, 10.1130/g22289.1, 2006.
- 538 Cheng, H., Fleitmann, D., Edwards, R. L., Wang, X., Cruz, F. W., Auler, A. S., Mangini, A., Wang, Y., Kong, X.,  
539 Burns, S. J., and Matter, A.: Timing and structure of the 8.2 kyr B.P. event inferred from  $\delta^{18}O$  records of  
540 stalagmites from China, Oman, and Brazil, *Geology*, 37, 1007-1010, 10.1130/G30126A.1, 2009.
- 541 Cheng, H., Sinha, A., Cruz, F. W., Wang, X., Edwards, R. L., d'Horta, F. M., Ribas, C. C., Vuille, M., Stott, L.  
542 D., and Auler, A. S.: Climate change patterns in Amazonia and biodiversity, *Nature Communications*, 4,  
543 1411, 10.1038/ncomms2415, 2013.
- 544 Cheng, H., Springer, G. S., Sinha, A., Hardt, B. F., Yi, L., Li, H., Tian, Y., Li, X., Rowe, H. D., Kathayat, G., Ning,  
545 Y., and Edwards, R. L.: Eastern North American climate in phase with fall insolation throughout the last  
546 three glacial-interglacial cycles, *Earth and Planetary Science Letters*, 522, 125-134,  
547 10.1016/j.epsl.2019.06.029, 2019.
- 548 Columbu, A., Spötl, C., De Waele, J., Yu, T.-L., Shen, C.-C., and Gázquez, F.: A long record of MIS 7 and MIS  
549 5 climate and environment from a western Mediterranean speleothem (SW Sardinia, Italy), *Quaternary  
550 Science Reviews*, 220, 230-243, 10.1016/J.QUASCIREV.2019.07.023, 2019.
- 551 Comas-Bru, L., and Harrison, S. P.: SISAL: Bringing added value to speleothem research, *Quaternary*, 2, 7,  
552 10.3390/quat2010007, 2019.
- 553 Comas-Bru, L., Harrison, S. P., Werner, M., Rehfeld, K., Scroxton, N., Veiga-Pires, C., and SISAL Working  
554 Group members: Evaluating model outputs using integrated global speleothem records of climate change  
555 since the last glacial, *Climate of the Past*, 15, 1557-1579, 10.5194/cp-15-1557-2019, 2019.
- 556 Comas-Bru, L., Atsawawanunt, K., Harrison, S.P. and SISAL Working Group members: SISAL (Speleothem  
557 Isotopes Synthesis and AnaLysis Working Group) database version 2.0. University of Reading. Dataset.  
558 <http://dx.doi.org/10.17864/1947.242>, 2020



- 559 Cruz, F. W., Burns, S. J., Karmann, I., Sharp, W. D., and Vuille, M.: Reconstruction of regional atmospheric  
560 circulation features during the late Pleistocene in subtropical Brazil from oxygen isotope composition of  
561 speleothems, *Earth and Planetary Science Letters*, 248, 495-507, 10.1016/J.EPSL.2006.06.019, 2006.
- 562 Czuppon, G., Demeny, A., Leel-Ossy, S., Ovari, M., Molnar, M., Stieber, J., Kiss, K., Karman, K., Suranyi, G.,  
563 and Haszpra, L.: Cave monitoring in the Beke and Baradla caves (Northeastern Hungary): implications for  
564 the conditions for the formation cave carbonates, *International Journal of Speleology*, 47, 13-28,  
565 10.5038/1827-806x.47.1.2110, 2018.
- 566 Deininger, M., Ward, M. B., Novello, F. V., and Cruz, W. F.: Late Quaternary Variations in the South  
567 American Monsoon System as Inferred by Speleothems—New Perspectives Using the SISAL Database,  
568 *Quaternary*, 2, 10.3390/quat2010006, 2019.
- 569 Demény, A., Kern, Z., Németh, A., Frisia, S., Hatvani, I. G., Czuppon, G., Leél-Őssy, S., Molnár, M., Óvári,  
570 M., Surányi, G., Gilli, A., Wu, C.-C., and Shen, C.-C.: North Atlantic influences on climate conditions in East-  
571 Central Europe in the late Holocene reflected by flowstone compositions, *Quaternary International*, 512,  
572 99-112, 10.1016/J.QUAINT.2019.02.014, 2019.
- 573 Denniston, R. F., Asmerom, Y., Lachniet, M., Polyak, V. J., Hope, P., An, N., Rodzinyak, K., and Humphreys,  
574 W. F.: A Last Glacial Maximum through middle Holocene stalagmite record of coastal Western Australia  
575 climate, *Quaternary Science Reviews*, 77, 101-112, 10.1016/j.quascirev.2013.07.002, 2013a.
- 576 Denniston, R. F., Wyrwoll, K.-H., Polyak, V. J., Brown, J. R., Asmerom, Y., Wanamaker, A. D., LaPointe, Z.,  
577 Ellerbroek, R., Barthelmes, M., Cleary, D., Cugley, J., Woods, D., and Humphreys, W. F.: A Stalagmite record  
578 of Holocene Indonesian–Australian summer monsoon variability from the Australian tropics, *Quaternary  
579 Science Reviews*, 78, 155-168, 10.1016/J.QUASCIREV.2013.08.004, 2013b.
- 580 Denniston, R. F., Asmerom, Y., Polyak, V. J., Wanamaker, A. D., Ummenhofer, C. C., Humphreys, W. F.,  
581 Cugley, J., Woods, D., and Lucker, S.: Decoupling of monsoon activity across the northern and southern  
582 Indo-Pacific during the Late Glacial, *Quaternary Science Reviews*, 176, 101-105,  
583 10.1016/J.QUASCIREV.2017.09.014, 2017a.
- 584 Denniston, R. F., Houts, A. N., Asmerom, Y., Wanamaker, A. D., Haws, J. A., Polyak, V. J., Thatcher, D. L.,  
585 Altan-Ochir, S., Borowske, A. C., Breitenbach, S. F. M., Ummenhofer, C. C., Regala, F. T., Benedetti, M. M.,  
586 and Bicho, N.: A Stalagmite Test of North Atlantic SST and Iberian Hydroclimate Linkages over the Last  
587 Two Glacial Cycles, *Climate of the Past Discussions*, 14, 1893-1913, 10.5194/cp-2017-146, 2017b.
- 588 Dong, J., Shen, C.-C., Kong, X., Wu, C.-C., Hu, H.-M., Ren, H., and Wang, Y.: Rapid retreat of the East Asian  
589 summer monsoon in the middle Holocene and a millennial weak monsoon interval at 9 ka in northern  
590 China, *Journal of Asian Earth Sciences*, 151, 31-39, 10.1016/J.JSEAES.2017.10.016, 2018.
- 591 Dumitru, O. A., Onac, B. P., Polyak, V. J., Wynn, J. G., Asmerom, Y., and Fornos, J. J.: Climate variability in  
592 the western Mediterranean between 121 and 67 ka derived from a Mallorcan speleothem record,  
593 *Palaeogeography Palaeoclimatology Palaeoecology*, 506, 128-138, 10.1016/j.palaeo.2018.06.028, 2018.
- 594 El-Shenawy, M. I., Kim, S. T., Schwarcz, H. P., Asmerom, Y., and Polyak, V. J.: Speleothem evidence for the  
595 greening of the Sahara and its implications for the early human dispersal out of sub-Saharan Africa,  
596 *Quaternary Science Reviews*, 188, 67-76, 10.1016/j.quascirev.2018.03.016, 2018.
- 597 Fleitmann, D., Cheng, H., Badertscher, S., Edwards, R. L., Mudelsee, M., Göktürk, O. M., Fankhauser, A.,  
598 Pickering, R., Raible, C. C., Matter, A., Kramers, J., and Tüysüz, O.: Timing and climatic impact of Greenland  
599 interstadials recorded in stalagmites from northern Turkey, *Geophysical Research Letters*, 36, L19707-  
600 L19707, 10.1029/2009GL040050, 2009.



- 601 Flohr, P., Fleitmann, D., Zorita, E., Sadekov, A., Cheng, H., Bosomworth, M., Edwards, L., Matthews, W.,  
602 and Matthews, R.: Late Holocene droughts in the Fertile Crescent recorded in a speleothem from northern  
603 Iraq, *Geophysical Research Letters*, 44, 1528-1536, 10.1002/2016GL071786, 2017.
- 604 Frappier, A., Sahagian, D., González, L. A., and Carpenter, S. J.: El Niño Events Recorded by Stalagmite  
605 Carbon Isotopes, *Science*, 298, 565-565, 10.1126/science.1076446, 2002.
- 606 Frappier, A. B., Sahagian, D., Carpenter, S. J., Gonzalez, L. A., and Frappier, B. R.: Stalagmite stable isotope  
607 record of recent tropical cyclone events, *Geology*, 35, 111-114, 10.1130/g23145a.1, 2007.
- 608 Gautam, P. K., Narayana, A. C., Band, S. T., Yadava, M. G., Ramesh, R., Wu, C.-C., and Shen, C.-C.: High-  
609 resolution reconstruction of Indian summer monsoon during the Bølling-Allerød from a central Indian  
610 stalagmite, *Palaeogeography, Palaeoclimatology, Palaeoecology*, 514, 567-576,  
611 10.1016/J.PALAEO.2018.11.006, 2019.
- 612 Göktürk, O. M., Fleitmann, D., Badertscher, S., Cheng, H., Edwards, R. L., Leuenberger, M., Fankhauser, A.,  
613 Tüysüz, O., and Kramers, J.: Climate on the southern Black Sea coast during the Holocene: implications  
614 from the Sofular Cave record, *Quaternary Science Reviews*, 30, 2433-2445,  
615 10.1016/J.QUASCIREV.2011.05.007, 2011.
- 616 Haslett, J., and Parnell, A.: A simple monotone process with application to radiocarbon-dated depth  
617 chronologies, *Journal of the Royal Statistical Society: Series C (Applied Statistics)*, 57, 399-418, 2008.
- 618 Hu, J, Emile-Geay J., and Partin J.: Correlation-based interpretations of paleoclimate data—where statistics  
619 meet past climates. *Earth and Planetary Science Letters* 459, 362-371, 2017.
- 620 Huguet, C., Routh, J., Fietz, S., Lone, M. A., Kalpana, M. S., Ghosh, P., Mangini, A., Kumar, V., and  
621 Rangarajan, R.: Temperature and Monsoon Tango in a Tropical Stalagmite: Last Glacial-Interglacial Climate  
622 Dynamics, *Scientific Reports*, 8, 5386, 10.1038/s41598-018-23606-w, 2018.
- 623 Isola, I., Zanchetta, G., Drysdale, R. N., Regattieri, E., Bini, M., Bajo, P., Hellstrom, J. C., Baneschi, I., Lionello,  
624 P., Woodhead, J., and Greig, A.: The 4.2 ka event in the central Mediterranean: New data from a Corchia  
625 speleothem (Apuan Alps, central Italy), *Climate of the Past*, 15, 135-151, 10.5194/cp-15-135-2019, 2019.
- 626 Jamieson, R. A., Baldini, J. U. L., Frappier, A. B., and Müller, W.: Volcanic ash fall events identified using  
627 principal component analysis of a high-resolution speleothem trace element dataset, *Earth and Planetary  
628 Science Letters*, 426, 36-45, 10.1016/J.EPSL.2015.06.014, 2015.
- 629 Jex, C. N., Baker, A., Fairchild, I. J., Eastwood, W. J., Leng, M. J., Sloane, H. J., Thomas, L., and Bekaroglu,  
630 E.: Calibration of speleothem delta O-18 with instrumental climate records from Turkey, *Global and  
631 Planetary Change*, 71, 207-217, 10.1016/j.gloplacha.2009.08.004, 2010.
- 632 Jex, C. N., Baker, A., Eden, J. M., Eastwood, W. J., Fairchild, I. J., Leng, M. J., Thomas, L., and Sloane, H. J.:  
633 A 500 yr speleothem-derived reconstruction of late autumn-winter precipitation, northeast Turkey,  
634 *Quaternary Research*, 75, 399-405, 10.1016/j.yqres.2011.01.005, 2011.
- 635 Jex, C. N., Phipps, S. J., Baker, A., and Bradley, C.: Reducing uncertainty in the climatic interpretations of  
636 speleothem delta O-18, *Geophysical Research Letters*, 40, 2259-2264, 10.1002/grl.50467, 2013.
- 637 Jiang, X., He, Y., Shen, C., Kong, X., Li, Z., and Chang, Y.: Stalagmite-inferred Holocene precipitation in  
638 northern Guizhou Province, China, and asynchronous termination of the Climatic Optimum in the Asian  
639 monsoon territory, *Chinese Science Bulletin*, 57, 795-801, 10.1007/s11434-011-4848-6, 2012.





- 640 Jiang, X., He, Y., Shen, C.-C., Li, Z., and Lin, K.: Replicated stalagmite-inferred centennial-to decadal-scale  
641 monsoon precipitation variability in southwest China since the mid Holocene, *The Holocene*, 23, 841-849,  
642 10.1177/0959683612471986, 2013.
- 643 Jo, K.-n., Yi, S., Lee, J.-Y., Woo, K. S., Cheng, H., Edwards, L. R., and Kim, S.-T.: 1000-Year Quasi-Periodicity  
644 of Weak Monsoon Events in Temperate Northeast Asia since the Mid-Holocene, *Scientific Reports*, 7,  
645 15196, 10.1038/s41598-017-15566-4, 2017.
- 646 Johnson, K. R., Ingram, B. L., Sharp, W. D., and Zhang, P. Z.: East Asian summer monsoon variability during  
647 Marine Isotope Stage 5 based on speleothem  $\delta^{18}\text{O}$  records from Wanxiang Cave, central China,  
648 *Palaeogeography Palaeoclimatology Palaeoecology*, 236, 5-19, 10.1016/j.palaeo.2005.11.041, 2006.
- 649 Kanner, L. C., Burns, S. J., Cheng, H., and Edwards, R. L.: High-Latitude Forcing of the South American  
650 Summer Monsoon During the Last Glacial, *Science*, 335, 570-573, 10.1126/science.1213397, 2012.
- 651 Kanner, L. C., Burns, S. J., Cheng, H., Edwards, R. L., and Vuille, M.: High-resolution variability of the South  
652 American summer monsoon over the last seven millennia: insights from a speleothem record from the  
653 central Peruvian Andes, *Quaternary Science Reviews*, 75, 1-10, 10.1016/j.quascirev.2013.05.008, 2013.
- 654 Kathayat, G., Cheng, H., Sinha, A., Yi, L., Li, X. L., Zhang, H. W., Li, H. Y., Ning, Y. F., and Edwards, R. L.: The  
655 Indian monsoon variability and civilization changes in the Indian subcontinent, *Science Advances*, 3,  
656 e1701296, 10.1126/sciadv.1701296, 2017.
- 657 Kathayat, G., Cheng, H., Sinha, A., Berkelhammer, M., Zhang, H., Duan, P., Li, H., Li, X., Ning, Y., and  
658 Edwards, R. L.: Evaluating the timing and structure of the 4.2 ka event in the Indian summer monsoon  
659 domain from an annually resolved speleothem record from Northeast India, *Climate of the Past*, 14, 1869-  
660 1879, 10.5194/cp-14-1869-2018, 2018.
- 661 Kaushal, N., Breitenbach, F. M. S., Lechleitner, A. F., Sinha, A., Tewari, C. V., Ahmad, M. S., Berkelhammer,  
662 M., Band, S., Yadava, M., Ramesh, R., and Henderson, M. G.: The Indian Summer Monsoon from a  
663 Speleothem  $\delta^{18}\text{O}$  Perspective—A Review, *Quaternary*, 1, 29, 10.3390/quat1030029, 2018.
- 664 Kern, Z., Demény, A., Perşoiu, A., and Hatvani, G. I.: Speleothem Records from the Eastern Part of Europe  
665 and Turkey—Discussion on Stable Oxygen and Carbon Isotopes, *Quaternary*, 2, 10.3390/quat2030031,  
666 2019.
- 667 Krause, C. E., Gagan, M. K., Dunbar, G. B., Hantoro, W. S., Hellstrom, J. C., Cheng, H., Edwards, R. L.,  
668 Suwargadi, B. W., Abram, N. J., and Rifai, H.: Spatio-temporal evolution of Australasian monsoon  
669 hydroclimate over the last 40,000 years, *Earth and Planetary Science Letters*, 513, 103-112,  
670 10.1016/J.EPSL.2019.01.045, 2019.
- 671 Lachniet, M. S., Asmerom, Y., Burns, S. J., Patterson, W. P., Polyak, V. J., and Seltzer, G. O.: Tropical  
672 response to the 8200 yr BP cold event? Speleothem isotopes indicate a weakened early Holocene  
673 monsoon in Costa Rica, *Geology*, 32, 957-960, 10.1130/g20797.1, 2004.
- 674 Lachniet, M. S., Johnson, L., Asmerom, Y., Burns, S. J., Polyak, V., Patterson, W. P., Burt, L., and Azouz, A.:  
675 Late Quaternary moisture export across Central America and to Greenland: evidence for tropical rainfall  
676 variability from Costa Rican stalagmites, *Quaternary Science Reviews*, 28, 3348-3360,  
677 10.1016/J.QUASCIREV.2009.09.018, 2009.
- 678 Laskar, A. H., Yadava, M. G., Ramesh, R., Polyak, V. J., and Asmerom, Y.: A 4 kyr stalagmite oxygen isotopic  
679 record of the past Indian Summer Monsoon in the Andaman Islands, *Geochemistry, Geophysics,*  
680 *Geosystems*, 14, 3555-3566, 10.1002/ggge.20203, 2013.



- 681 Lauritzen, S.-E., and Onac, B. P.: Isotopic Stratigraphy of a Last Interglacial Stalagmite from Northwestern  
682 Romania: Correlation with the Deep-Sea record and Northern-Latitude Speleothem, *Journal of Cave and*  
683 *Karst Studies*, 61, 22-30, 1999.
- 684 Lechleitner, F. A., Amirnezhad-Mozhdehi, S., Columbu, A., Comas-Bru, L., Labuhn, I., Pérez-Mejías, C., and  
685 Rehfeld, K.: The Potential of Speleothems from Western Europe as Recorders of Regional Climate: A  
686 Critical Assessment of the SISAL Database, *Quaternary*, 1, <https://doi.org/10.3390/quat1030030>, 2018.
- 687 Li, H., Cheng, H., Sinha, A., Kathayat, G., Spötl, C., André, A. A., Meunier, A., Biswas, J., Duan, P., Ning, Y.,  
688 and Edwards, R. L.: Hydro-climatic variability in the southwestern Indian Ocean between 6000 and 3000  
689 years ago, *Climate of the Past*, 14, 1881-1891, 10.5194/cp-14-1881-2018, 2018.
- 690 Liu, X., Rao, Z., Shen, C. C., Liu, J., Chen, J., Chen, S., Wang, X., and Chen, F.: Holocene Solar Activity Imprint  
691 on Centennial- to Multidecadal-Scale Hydroclimatic Oscillations in Arid Central Asia, *Journal of*  
692 *Geophysical Research: Atmospheres*, 124, 2562-2573, 10.1029/2018JD029699, 2019.
- 693 Logan, A. J.: A new paleoclimate record for North Westland, New Zealand, with implications for the  
694 interpretation of speleothem based paleoclimate proxies, Master of Science, Geology, University of  
695 Canterbury, 109 pp., 2011.
- 696 Lončar, N., Bar-Matthews, M., Ayalon, A., Faivre, S., and Surić, M.: Holocene climatic conditions in the  
697 eastern Adriatic recorded in stalagmites from Strašna peć Cave (Croatia), *Quaternary International*, 508,  
698 98-106, 10.1016/j.quaint.2018.11.006, 2019.
- 699 Lorrey, A., Williams, P., Salinger, J., Martin, T., Palmer, J., Fowler, A., Zhao, J.-x., and Neil, H.: Speleothem  
700 stable isotope records interpreted within a multi-proxy framework and implications for New Zealand  
701 palaeoclimate reconstruction, *Quaternary International*, 187, 52-75, 10.1016/j.quaint.2007.09.039, 2008.
- 702 Marsh, A., Fleitmann, D., Al-Manmi, D. A. M., Altaweel, M., Wengrow, D., and Carter, R.: Mid- to late-  
703 Holocene archaeology, environment and climate in the northeast Kurdistan region of Iraq, *The Holocene*,  
704 28, 955-967, 10.1177/0959683617752843, 2018.
- 705 McCabe-Glynn, S., Johnson, K. R., Strong, C., Berkelhammer, M., Sinha, A., Cheng, H., and Edwards, R. L.:  
706 Variable North Pacific influence on drought in southwestern North America since AD 854, *Nature*  
707 *Geoscience*, 6, 617-621, 10.1038/ngeo1862, 2013.
- 708 Medina-Elizalde, M., Burns, S. J., Polanco-Martinez, J. M., Beach, T., Lases-Hernandez, F., Shen, C. C., and  
709 Wang, H. C.: High-resolution speleothem record of precipitation from the Yucatan Peninsula spanning the  
710 Maya Preclassic Period, *Global and Planetary Change*, 138, 93-102, 10.1016/j.gloplacha.2015.10.003,  
711 2016.
- 712 Medina-Elizalde, M., Burns, S. J., Polanco-Martinez, J., Lases-Hernandez, F., Bradley, R., Wang, H. C., and  
713 Shen, C. C.: Synchronous precipitation reduction in the American Tropics associated with Heinrich 2,  
714 *Scientific Reports*, 7, 10.1038/s41598-017-11742-8, 2017.
- 715 Moseley, G. E., Spötl, C., Brandstätter, S., Erhardt, T., Luetscher, M., and Edwards, R. L.: NALPS19: Sub-  
716 orbital scale climate variability recorded in Northern Alpine speleothems during the last glacial period,  
717 *Climate of the Past*, 16, 29-50, 10.5194/cp-16-19-2020, 2020.
- 718 Mudelsee, M., Fohlmeister, J. and Scholz, D.: Effects of dating errors on nonparametric trend analyses of  
719 speleothem time series, *Climate of the Past*, 8, 1637-1648, 10.5194/cp-8-1637-2012, 2012.
- 720 Niggemann, S., Mangini, A., Mudelsee, M., Richter, D. K., and Wurth, G.: Sub-Milankovitch climatic cycles  
721 in Holocene stalagmites from Sauerland, Germany, *Earth and Planetary Science Letters*, 216, 539-547,  
722 10.1016/S0012-821X(03)00513-2, 2003a.



- 723 Niggemann, S., Mangini, A., Richter, D. K., and Wurth, G.: A paleoclimate record of the last 17,600 years  
724 in stalagmites from the B7 cave, Sauerland, Germany, *Quaternary Science Reviews*, 22, 555-567,  
725 10.1016/s0277-3791(02)00143-9, 2003b.
- 726 Osete, M. L., Martin-Chivelet, J., Rossi, C., Edwards, R. L., Egli, R., Munoz-Garcia, M. B., Wang, X. F., Pavon-  
727 Carrasco, F. J., and Heller, F.: The Blake geomagnetic excursion recorded in a radiometrically dated  
728 speleothem, *Earth and Planetary Science Letters*, 353, 173-181, 10.1016/j.epsl.2012.07.041, 2012.
- 729 Oster, J. L., Warken, S. F., Sekhon, N., Arienzo, M., and Lachniet, M.: Speleothem Paleoclimatology for the  
730 Caribbean, Central America, and North America, *Quaternary*, 2, 10.3390/quat2010005, 2019.
- 731 Parnell, A.: Bchron: Radiocarbon dating, age-depth modelling, relative sea level rate estimation, and non-  
732 parametric phase modelling, R package version 4.3.0., 2018.
- 733 Partin, J. W., Quinn, T. M., Shen, C. C., Okumura, Y., Cardenas, M. B., Siringan, F. P., Banner, J. L., Lin, K.,  
734 Hu, H. M., and Taylor, F. W.: Gradual onset and recovery of the Younger Dryas abrupt climate event in the  
735 tropics, *Nature Communications*, 6, 8061-8061, 10.1038/ncomms9061, 2015.
- 736 Pawlak, J., Błaszczak, M., Hercman, H., and Matoušková, Š.: A continuous stable isotope record of last  
737 interglacial age from the Bulgarian Cave Orlova Chuka, *Geochronometria*, 46, 87-101, 10.1515/geochr-  
738 2015-0107, 2019.
- 739 Peckover, E. N., Andrews, J. E., Leeder, M. R., Rowe, P. J., Marca, A., Sahy, D., Noble, S., and Gawthorpe,  
740 R.: Coupled stalagmite – Alluvial fan response to the 8.2 ka event and early Holocene palaeoclimate  
741 change in Greece, *Palaeogeography, Palaeoclimatology, Palaeoecology*, 532, 109252-109252,  
742 10.1016/j.palaeo.2019.109252, 2019.
- 743 Polyak, V. J., Asmerom, Y., and Lachniet, M. S.: Rapid speleothem  $\delta^{13}\text{C}$  change in southwestern North  
744 America coincident with Greenland stadial 20 and the Toba (Indonesia) supereruption, *Geology*, 45, 843-  
745 846, 10.1130/g39149.1, 2017.
- 746 R Core Team: R: A language and environment for statistical computing. R Foundation for Statistical  
747 Computing, Vienna, Austria, <http://www.r-project.org/index.html>, 2019.
- 748 Rehfeld, K., and Kurths, J.: Similarity estimators for irregular and age-uncertain time series, *Climate of the  
749 Past*, 10, 107-122, 2014.
- 750 Rivera-Collazo, I., Winter, A., Scholz, D., Mangini, A., Miller, T., Kushnir, Y., and Black, D.: Human  
751 adaptation strategies to abrupt climate change in Puerto Rico ca. 3.5 ka, *Holocene*, 25, 627-640,  
752 10.1177/0959683614565951, 2015.
- 753 Roesch, C., and Rehfeld, K.: Automatising construction and evaluation of age-depth models for hundreds  
754 of speleothems, 9th International Workshop on Climate Informatics, 2019.
- 755 Rossi, C., Mertz-Kraus, R., and Osete, M. L.: Paleoclimate variability during the Blake geomagnetic  
756 excursion (MIS 5d) deduced from a speleothem record, *Quaternary Science Reviews*, 102, 166-180,  
757 10.1016/j.quascirev.2014.08.007, 2014.
- 758 Rossi, C., Bajo, P., Lozano, R. P., and Hellstrom, J.: Younger Dryas to Early Holocene paleoclimate in  
759 Cantabria (N Spain): Constraints from speleothem Mg, annual fluorescence banding and stable isotope  
760 records, *Quaternary Science Reviews*, 192, 71-85, 10.1016/j.quascirev.2018.05.025, 2018.



- 761 Rudzka-Phillips, D., McDermott, F., Jackson, A., and Fleitmann, D.: Inverse modelling of the C-14 bomb  
762 pulse in stalagmites to constrain the dynamics of soil carbon cycling at selected European cave sites,  
763 *Geochimica et Cosmochimica Acta*, 112, 32-51, 10.1016/j.gca.2013.02.032, 2013.
- 764 Rudzka, D., McDermott, F., and Suric, M.: A late Holocene climate record in stalagmites from Modric Cave  
765 (Croatia), *Journal of Quaternary Science*, 27, 585-596, 10.1002/jqs.2550, 2012.
- 766 Scholz, D., and Hoffmann, D. L.: StalAge - An algorithm designed for construction of speleothem age  
767 models, *Quaternary Geochronology*, 6, 369-382, 10.1016/j.quageo.2011.02.002, 2011.
- 768 Scroxton, N., Burns, S. J., McGee, D., Hardt, B., Godfrey, L. R., Ranivoharimanana, L., and Faina, P.:  
769 Competing Temperature and Atmospheric Circulation Effects on Southwest Madagascan Rainfall During  
770 the Last Deglaciation, *Paleoceanography and Paleoclimatology*, 34, 275-286, 10.1029/2018PA003466,  
771 2019.
- 772 Sinha, N., Gandhi, N., Chakraborty, S., Krishnan, R., Yadava, M. G., and Ramesh, R.: Abrupt climate change  
773 at ~2800 yr BP evidenced by a stalagmite record from peninsular India, *The Holocene*, 28, 1720-1730,  
774 10.1177/0959683618788647, 2018.
- 775 Staubwasser, M., Drăgușin, V., Onac, B. P., Assonov, S., Ersek, V., Hoffmann, D. L., and Veres, D.: Impact  
776 of climate change on the transition of Neanderthals to modern humans in Europe, *Proceedings of the  
777 National Academy of Sciences of the United States of America*, 115, 9116-9121,  
778 10.1073/pnas.1808647115, 2018.
- 779 Steponaitis, E., Andrews, A., McGee, D., Quade, J., Hsieh, Y. T., Broecker, W. S., Shuman, B. N., Burns, S. J.,  
780 and Cheng, H.: Mid-Holocene drying of the US Great Basin recorded in Nevada speleothems, *Quaternary  
781 Science Reviews*, 127, 174-185, 10.1016/j.quascirev.2015.04.011, 2015.
- 782 Strikis, N. M., Chiessi, C. M., Cruz, F. W., Vuille, M., Cheng, H., Barreto, E. A. D., Mollenhauer, G., Kasten,  
783 S., Karmann, I., Edwards, R. L., Bernal, J. P., and Sales, H. D.: Timing and structure of Mega-SACZ events  
784 during Heinrich Stadial 1, *Geophysical Research Letters*, 42, 5477-5484, 10.1002/2015gl064048, 2015.
- 785 Stríkis, N. M., Cruz, F. W., Barreto, E. A. S., Naughton, F., Vuille, M., Cheng, H., Voelker, A. H. L., Zhang, H.,  
786 Karmann, I., Edwards, R. L., Auler, A. S., Santos, R. V., and Sales, H. R.: South American monsoon response  
787 to iceberg discharge in the North Atlantic, *Proceedings of the National Academy of Sciences of the United  
788 States of America*, 115, 3788-3793, 10.1073/pnas.1717784115, 2018.
- 789 Talma, A. S. and Vogel, J. C.: Late Quaternary Paleotemperatures Derived from a Speleothem from Cango  
790 Caves, Cape Province, South Africa, *Quaternary Research*, 37(2), 203-213, 10.1016/0033-5894(92)90082-  
791 t, 1992.
- 792 Tan, L., An, Z., Huh, C.-A., Cai, Y., Shen, C.-C., Shiao, L.-J., Yan, L., Cheng, H., and Edwards, R. L.: Cyclic  
793 precipitation variation on the western Loess Plateau of China during the past four centuries, *Scientific  
794 Reports*, 4, 6381-6381, 10.1038/srep06381, 2015.
- 795 Tan, L., Cai, Y., Cheng, H., Edwards, L. R., Gao, Y., Xu, H., Zhang, H., and An, Z.: Centennial- to decadal-scale  
796 monsoon precipitation variations in the upper Hanjiang River region, China over the past 6650 years, *Earth  
797 and Planetary Science Letters*, 482, 580-590, 10.1016/j.epsl.2017.11.044, 2018a.
- 798 Tan, L., Cai, Y., Cheng, H., Edwards, L. R., Lan, J., Zhang, H., Li, D., Ma, L., Zhao, P., and Gao, Y.: High  
799 resolution monsoon precipitation changes on southeastern Tibetan Plateau over the past 2300 years,  
800 *Quaternary Science Reviews*, 195, 122-132, 10.1016/J.QUASCIREV.2018.07.021, 2018b.



- 801 Tzedakis, P. C., Drysdale, R. N., Margari, V., Skinner, L. C., Menviel, L., Rhodes, R. H., Taschetto, A. S.,  
802 Hodell, D. A., Crowhurst, S. J., Hellstrom, J. C., Fallick, A. E., Grimalt, J. O., McManus, J. F., Martrat, B.,  
803 Mokeddem, Z., Parrenin, F., Regattieri, E., Roe, K., and Zanchetta, G.: Enhanced climate instability in the  
804 North Atlantic and southern Europe during the Last Interglacial, *Nature Communications*, 9, 4235-4235,  
805 10.1038/s41467-018-06683-3, 2018.
- 806 van Breukelen, M. R., Vonhof, H. B., Hellstrom, J. C., Wester, W. C. G., and Kroon, D.: Fossil dripwater in  
807 stalagmites reveals Holocene temperature and rainfall variation in Amazonia, *Earth and Planetary Science*  
808 *Letters*, 275, 54-60, 10.1016/J.EPSL.2008.07.060, 2008.
- 809 Van Rempelbergh, M., Fleitmann, D., Verheyden, S., Cheng, H., Edwards, L., De Geest, P., De  
810 Vleeschouwer, D., Burns, S. J., Matter, A., Claeys, P., and Keppens, E.: Mid- to late Holocene Indian Ocean  
811 Monsoon variability recorded in four speleothems from Socotra Island, Yemen, *Quaternary Science*  
812 *Reviews*, 65, 129-142, 10.1016/j.quascirev.2013.01.016, 2013.
- 813 Verheyden, S., Keppens, E., Fairchild, I. J., McDermott, F., and Weis, D.: Mg, Sr and Sr isotope geochemistry  
814 of a Belgian Holocene speleothem: implications for paleoclimate reconstructions, *Chemical Geology*, 169,  
815 131-144, 10.1016/S0009-2541(00)00299-0, 2000.
- 816 Verheyden, S., Keppens, E., Quinif, Y., Cheng, H. J., and Edwards, L. R.: Late-glacial and Holocene climate  
817 reconstruction as inferred from a stalagmite-Grotte du Père Noël, Han-sur-Lesse, Belgium, *Geologica*  
818 *Belgica*, 17, 83-89, <https://popups.uliege.be/1374-8505/index.php?id=4421&file=1&pid=4412>, 2014.
- 819 Wang, J. K., Johnson, K. R., Borsato, A., Amaya, D. J., Griffiths, M. L., Henderson, G. M., Frisia, S., and  
820 Mason, A.: Hydroclimatic variability in Southeast Asia over the past two millennia, *Earth and Planetary*  
821 *Science Letters*, 525, 115737-115737, 10.1016/j.epsl.2019.115737, 2019.
- 822 Wang, Y. J., Cheng, H., Edwards, R. L., Kong, X. G., Shao, X. H., Chen, S. T., Wu, J. Y., Jiang, X. Y., Wang, X.  
823 F., and An, Z. S.: Millennial- and orbital-scale changes in the East Asian monsoon over the past 224,000  
824 years, *Nature*, 451, 1090-1093, 10.1038/nature06692, 2008.
- 825 Ward, B. M., Wong, C. I., Novello, V. F., McGee, D., Santos, R. V., Silva, L. C. R., Cruz, F. W., Wang, X.,  
826 Edwards, R. L., and Cheng, H.: Reconstruction of Holocene coupling between the South American  
827 Monsoon System and local moisture variability from speleothem  $\delta^{18}\text{O}$  and  $^{87}\text{Sr}/^{86}\text{Sr}$  records, *Quaternary*  
828 *Science Reviews*, 210, 51-63, 10.1016/J.QUASCIREV.2019.02.019, 2019.
- 829 Warken, S. F., Fohlmeister, J., Schröder-Ritzrau, A., Constantin, S., Spötl, C., Gerdes, A., Esper, J., Frank, N.,  
830 Arps, J., Terente, M., Riechelmann, D. F. C., Mangini, A. and Scholz, D.: Reconstruction of late Holocene  
831 autumn/winter precipitation variability in SW Romania from a high-resolution speleothem trace element  
832 record, *Earth Planet. Sci. Lett.*, 499, 122-133, 10.1016/j.epsl.2018.07.027, 2018.
- 833 Warken, S. F., Scholz, D., Spötl, C., Jochum, K. P., Pajón, J. M., Bahr, A., and Mangini, A.: Caribbean  
834 hydroclimate and vegetation history across the last glacial period, *Quaternary Science Reviews*, 218, 75-  
835 90, 10.1016/J.QUASCIREV.2019.06.019, 2019.
- 836 Webb, M., Dredge, J., Barker, P. A., Muller, W., Jex, C., Desmarchelier, J., Hellstrom, J., and Wynn, P. M.:  
837 Quaternary climatic instability in south-east Australia from a multi-proxy speleothem record, *Journal of*  
838 *Quaternary Science*, 29, 589-596, 10.1002/jqs.2734, 2014.
- 839 Weber, M., Scholz, D., Schröder-Ritzrau, A., Deininger, M., Spötl, C., Lugli, F., Mertz-Kraus, R., Jochum, K.  
840 P., Fohlmeister, J., Stumpf, C. F., and Riechelmann, D. F. C.: Evidence of warm and humid interstadials in



- 841 central Europe during early MIS 3 revealed by a multi-proxy speleothem record, *Quaternary Science*  
842 *Reviews*, 200, 276-286, 10.1016/J.QUASCIREV.2018.09.045, 2018.
- 843 Wendt, K. A., Häuselmann, A. D., Fleitmann, D., Berry, A. E., Wang, X., Auler, A. S., Cheng, H., and Edwards,  
844 R. L.: Three-phased Heinrich Stadial 4 recorded in NE Brazil stalagmites, *Earth and Planetary Science*  
845 *Letters*, 510, 94-102, 10.1016/J.EPSL.2018.12.025, 2019.
- 846 Whittaker, T. E.: High-resolution speleothem-based palaeoclimate records from New Zealand reveal  
847 robust teleconnection to North Atlantic during MIS 1-4, Unpubl. PhD Thesis, The University of Waikato,  
848 2008.
- 849 Wilcox, P. S., Dorale, J. A., Baichtal, J. F., Spötl, C., Fowell, S. J., Edwards, R. L., and Kovarik, J. L.: Millennial-  
850 scale glacial climate variability in Southeastern Alaska follows Dansgaard-Oeschger cyclicity, *Scientific*  
851 *Reports*, 9, 7880-7880, 10.1038/s41598-019-44231-1, 2019.
- 852 Williams, P. W., King, D. N. T., Zhao, J. X., and Collerson, K. D.: Late pleistocene to holocene composite  
853 speleothem O-18 and C-13 chronologies from south island, new Zealand-did a global younger dryas really  
854 exist?, *Earth and Planetary Science Letters*, 230, 301-317, 10.1016/j.epsl.2004.10.024, 2005.
- 855 Williams, P. W., Neil, H. L., and Zhao, J. X.: Age frequency distribution and revised stable isotope curves  
856 for New Zealand speleothems: palaeoclimatic implications, *International Journal of Speleology*, 39, 99-  
857 112, 10.5038/1827-806x.39.2.5, 2010.
- 858 Wu, J. Y., Wang, Y. J., Cheng, H., Kong, X. G., and Liu, D. B.: Stable isotope and trace element investigation  
859 of two contemporaneous annually-laminated stalagmites from northeastern China surrounding the 8.2 ka  
860 event, *Climate of the Past*, 8, 1497-1507, 10.5194/cp-8-1497-2012, 2012.
- 861 Yadava, M. G., Ramesh, R., and Pant, G. B.: Past monsoon rainfall variations in peninsular India recorded  
862 in a 331-year-old speleothem, *Holocene*, 14, 517-524, 10.1191/0959683604hl728rp, 2004.
- 863 Yin, J. J., Li, H. C., Rao, Z. G., Shen, C. C., Mii, H. S., Pillutla, R. K., Hu, H. M., Li, Y. X., and Feng, X. H.:  
864 Variations of monsoonal rain and vegetation during the past millennium in Tianguai Mountain, North China  
865 reflected by stalagmite delta O-18 and delta C-13 records from Zhenzhu Cave, *Quaternary International*,  
866 447, 89-101, 10.1016/j.quaint.2017.06.039, 2017.
- 867 Zhang, H., Cheng, H., Cai, Y., Spötl, C., Kathayat, G., Sinha, A., Edwards, R. L., and Tan, L.: Hydroclimatic  
868 variations in southeastern China during the 4.2 ka event reflected by stalagmite records, *Climate of the*  
869 *Past*, 14, 1805-1817, 10.5194/cp-14-1805-2018, 2018a.
- 870 Zhang, H., Cheng, H., Spötl, C., Cai, Y., Sinha, A., Tan, L., Yi, L., Yan, H., Kathayat, G., Ning, Y., Li, X., Zhang,  
871 F., Zhao, J., and Edwards, R. L.: A 200-year annually laminated stalagmite record of precipitation  
872 seasonality in southeastern China and its linkages to ENSO and PDO, *Scientific Reports*, 8, 12344-12344,  
873 10.1038/s41598-018-30112-6, 2018b.
- 874 Zhang, H., Ait Brahim, Y., Li, H., Zhao, J., Kathayat, G., Tian, Y., Baker, J., Wang, J., Zhang, F., Ning, Y.,  
875 Edwards, L. R., and Cheng, H.: The Asian Summer Monsoon: Teleconnections and Forcing Mechanisms—  
876 A Review from Chinese Speleothem  $\delta^{18}\text{O}$  Records, *Quaternary*, 2, 10.3390/quat2030026, 2019.
- 877 Zhang, H. B., Griffiths, M. L., Huang, J. H., Cai, Y. J., Wang, C. F., Zhang, F., Cheng, H., Ning, Y. F., Hu, C. Y.,  
878 and Xie, S. C.: Antarctic link with East Asian summer monsoon variability during the Heinrich Stadial-Bølling  
879 interstadial transition, *Earth and Planetary Science Letters*, 453, 243-251, 10.1016/j.epsl.2016.08.008,  
880 2016.



- 881 Zhang, H. L., Yu, K. F., Zhao, J. X., Feng, Y. X., Lin, Y. S., Zhou, W., and Liu, G. H.: East Asian Summer Monsoon  
882 variations in the past 12.5 ka: High-resolution delta O-18 record from a precisely dated aragonite  
883 stalagmite in central China, *Journal of Asian Earth Sciences*, 73, 162-175, 10.1016/j.jseaes.2013.04.015,  
884 2013.
- 885 Zhang, P., Cheng, H., Edwards, R. L., Chen, F., Wang, Y., Yang, X., Liu, J., Tan, M., Wang, X., Liu, J., An, C.,  
886 Dai, Z., Zhou, J., Zhang, D., Jia, J., Jin, L., and Johnson, K. R.: A Test of Climate, Sun, and Culture Relationships  
887 from an 1810-Year Chinese Cave Record, *Science*, 322, 940-942, 10.1126/science.1163965, 2008.